# GENE TRANSCRIPTION PROFILE OF THE DETACHED RETINA (AN AOS THESIS)

BY David N. Zacks MD PhD

## ABSTRACT

*Purpose:* Separation of the neurosensory retina from the retinal pigment epithelium (RPE) yields many morphologic and functional consequences, including death of the photoreceptor cells, Müller cell hypertrophy, and inner retinal rewiring. Many of these changes are due to the separation-induced activation of specific genes. In this work, we define the gene transcription profile within the retina as a function of time after detachment. We also define the early activation of kinases that might be responsible for the detachment-induced changes in gene transcription.

*Methods:* Separation of the retina from the RPE was induced in Brown-Norway rats by the injection of 1% hyaluronic acid into the subretinal space. Retinas were harvested at 1, 7, and 28 days after separation. Gene transcription profiles for each time point were determined using the Affymetrix Rat 230A gene microarray chip. Transcription levels in detached retinas were compared to those of nondetached retinas with the BRB-ArrayTools Version 3.6.0 using a random variance analysis of variance (ANOVA) model. Confirmation of the significant transcriptional changes for a subset of the genes was performed using microfluidic quantitative real-time polymerase chain reaction (qRT-PCR) assays. Kinase activation was explored using Western blot analysis to look for early phosphorylation of any of the 3 main families of mitogen-activated protein kinases (MAPK): the p38 family, the Janus kinase family, and the p42/p44 family.

*Results:* Retinas separated from the RPE showed extensive alterations in their gene transcription profile. Many of these changes were initiated as early as 1 day after separation, with significant increases by 7 days. ANOVA analysis defined 144 genes that had significantly altered transcription levels as a function of time after separation when setting a false discovery rate at ≤0.1. Confirmatory RT-PCR was performed on 51 of these 144 genes. Differential transcription detected on the microarray chip was confirmed by qRT-PCR for all 51 genes. Western blot analysis showed that the p42/p44 family of MAPK was phosphorylated within 2 hours of retinal-RPE separation. This phosphorylation was detachment-induced and could be inhibited by specific inhibitors of MAPK phosphorylation.

*Conclusions:* Separation of the retina from the RPE induces significant alteration in the gene transcription profile within the retina. These profiles are not static, but change as a function of time after detachment. These gene transcription changes are preceded by the activation of the p42/p44 family of MAPK. This altered transcription may serve as the basis for many of the morphologic, biochemical, and functional changes seen within the detached retina.

*Trans Am Ophthalmol Soc 2009;107:343-382*

## INTRODUCTION

The retina is a complex, multilayered neural tissue that provides the first point of sensory transduction for visual stimuli.[1] The retina has multiple cell types, both neural and nonneural. These cells are arranged in a very specific and orderly manner, and their cellular function is very highly regulated. Metabolic support to the retina is complex and varies by species.[2,3] In the primate eye, there are 2 main vascular supplies. The retinal circulation provides nutritional support to the inner two-thirds of the retina from the outer plexiform layer to the internal limiting membrane. The outer retina (photoreceptor cell layer) receives its metabolic support from the underlying choroidal circulation via the retinal pigment epithelium (RPE).

A common form of injury to the retina is separation from the RPE—a phenomenon known as a retinal detachment. Retinal detachment has typically been thought of in the context of the rhegmatogenous retinal detachment. In 1904, Jules Gonin[4] published the first report describing the retinal tear as the cause of retinal detachment in 3 patients. Subsequent to the seminal work of Jules Gonin, however, it became apparent that separation of the retina from the RPE can occur in a wide variety of ocular conditions, and not just from a retinal tear (ie, the rhegmatogenous retinal detachment).[5] Retinal detachment can also occur when leakage of fluid into the subretinal space causes the retina to lift off of the RPE, a process known as an exudative or serous retinal detachment. Such leakage can be due to ocular inflammation, retinal or choroidal tumors, or the presence of abnormal blood vessels with leakage into the subretinal space (for example, the presence of a choroidal neovascular membrane). Retinal-RPE separation can also be caused by the formation of fibrous or fibrovascular bands that exert traction on the retina and elevate it from the RPE—a process known as the tractional retinal detachment. This process is typically seen in conditions such as proliferative diabetic retinopathy and proliferative vitreoretinopathy.

When the retina becomes separated from the RPE, there is a disruption in the normal homeostasis of the retina.[6] This results in significant morphologic, biochemical, and functional changes, such as photoreceptor cell death, Müller cell hypertrophy, and neuronal rewiring, all of which can contribute to permanent visual loss, even if the retina is reattached. One way in which cells respond to alterations in their homeostatic condition is by altering the types of genes they express.[7-10] These genes may code for stress-response proteins or for enzymes that can help the cell cope with the new surrounding conditions. If unchecked, however, the altered transcription profile may have deleterious effects on the overall function of the cells. It is the underlying hypothesis of this thesis that separation of the retina from the RPE causes the retina to transcribe genes that are different from those it would normally transcribe when attached. In this thesis, this hypothesis is tested by measuring the gene transcript levels in detached vs attached retinas as a function of time after detachment.

From the Kellogg Eye Center, University of Michigan, Ann Arbor.

## MORPHOLOGIC STUDIES OF RETINAL DETACHMENT

Some of the earliest descriptions of the morphologic changes that occur after retinal detachment appear in the writings of Drs Kroll and Machemer.[11-16] They created experimental retinal detachments in owl monkey eyes by aspirating vitreous and injecting it into the subretinal space. They proceeded to collect these eyes at various time points after creation of the detachment and then examined the eyes using light and electron microscopy. Using this technique, Kroll and Machemer showed that retinal detachment resulted in near complete disruption of the normal orderly array of rod and cone outer segments. The outer segments were sloughed off by the cells into the subretinal space, with subsequent degeneration and removal by infiltrating macrophages. Retinal detachment also resulted in the loss of photoreceptor cells as indicated by the thinning of the outer nuclear layer. The inner retina, too, was affected by retinal-RPE separation. Kroll and Machemer described the formation of cyst-like spaces within the outer plexiform and inner nuclear layers, as well as the disruption of the normal axon-dendrite pattern between photoreceptors and bipolar cells.

Pulse-label experiments using radiolabeled amino acids showed that attached retinas produced significant amounts of protein in their photoreceptors and that these proteins were preferentially targeted toward the outer segments.[17,18] Detachment resulted in the disruption of this flow of proteins, as the outer segments were no longer present. No conclusion could be made, though, as to whether unique proteins were being produced in detached photoreceptors, or whether there was simply a misdirecting of the normally produced proteins.

Kroll and Machemer also showed that RPE cells undergo significant changes after retinal detachment, with these cells showing retraction of their apical processes that normally project into the space between the photoreceptor outer segments. This is accompanied by migration of the melanin granules from their normal position in the apical zone of the RPE cell toward the cell's basal side. Pulse-labeled studies similar to those described above for the retina showed that there was also a significant detachment-induced proliferation of the RPE cells.[19]

This original set of data from Kroll and Machemer was mainly descriptive in nature, and the investigators were limited by the technology of the time to mostly microscopic analyses. It was only in the late 1970s and early 1980s that more molecular techniques such as immunohistochemistry were applied to the study of retinal detachments. During that time period, a new model of experimental retinal detachment was introduced by Steven Fisher from the University of California at Santa Barbara. Fisher devised a technique for creating experimental detachments by inserting a needle through the pars plana, crossing the vitreous, creating a small retinotomy, and injecting 1% hyaluronic acid into the subretinal space. Fisher and his colleagues worked mostly in cats' eyes, but this technique has since been applied to other animals, particularly the rat and the mouse. As in the work of Kroll and Machemer, Fisher and coworkers harvested the eyes at different time points after the detachment was created for examination. The extensive work of this group is covered in several excellent reviews,[6,20,21] and the reader is referred to these articles for a complete description of their results. Briefly, though, Fisher and colleagues showed that 5 main changes occur in the retina following separation from the RPE, all of which worsen with the duration of the detachment. First, there is retraction of the photoreceptor outer segments.[22-24] Second, there is death of photoreceptors.[25] Third, there is a rewiring of the intraretinal neuronal connections, presumably caused by the lack of appropriate sensory stimulation from the photoreceptors.[26,27] Fourth, there is a proliferation of nonneuronal cell types such as astrocytes and Müller cells, and even such cells as pericytes and endothelial cells.[28] Finally, there is extensive hypertrophy of the Müller cells, causing an intraretinal gliosis that can spread onto the preretinal and subretinal surfaces in chronic detachments.[29-31] Fisher's group also expanded on the initial work of Kroll and Machemer as it related to the RPE cells after retinal detachment, showing that there is a loss of normal RPE cell architecture and a proliferation and migration of RPE cells into the area of the detachment.[19]

Fisher and coworkers also began to describe some of the molecular changes that occurred within the retina as a result of separation from the RPE. In particular, they showed extensive changes in the types of proteins that were expressed within the Müller cells.[32-34] Most notably, there was a very significant detachment-induced increase in the levels of glial fibrillary acidic protein (GFAP) and vimentin within the Müller cells. In contrast, the expression of glutamine synthetase, cellular retinaldehyde-binding protein, cellular retinol-binding protein, and carbonic anhydrase C was suppressed in the Müller cell after retinal detachment.[32] These detachment-induced alterations in protein synthesis could also be modulated by external signals such as growth factors or oxygen.[35-40] Work from their laboratory also showed the early activation of growth factor receptors and intracellular kinases that are known regulators of transcription.[41] They were the first to suggest that retinal detachment resulted in gene transcriptional changes. Most of the changes they reported occurred in Müller cells, but some were localized to photoreceptor cells.

## PHOTORECEPTOR DEATH AFTER RETINAL DETACHMENT: APOPTOSIS AND ITS ROLE IN RETINAL DISEASE

Cell death is an inevitable consequence of cell life. However, the manner in which cells die is not always the same. Cell death can result from a variety of factors and, depending on the stimulus for death, usually occurs by one of two main mechanisms: necrosis or apoptosis.[42] Necrosis represents an uncontrolled death of a large group of cells stimulated by catastrophic events such as inflammation, ischemia, or infection. Cells that die by necrosis usually undergo a random breakdown of their internal protein and nucleic acid components as the cell is consumed by inflammation stimulated by the inciting event.

Apoptosis, on the other hand, is a controlled form of cell death that uses the cell's own molecular machinery to package itself for eventual removal by the normal constituents of the surrounding environment. Apoptosis can occur as a normal part of organ development. For example, embryonic retinas contain many more ganglion cells than those found in newborns. The "weeding out" of the ganglion cells is thought to occur by apoptosis that is induced by the removal of neurotrophic signals.[43] Apoptosis-mediated death can also be induced by various disease states, which cause the release of "molecular triggers" that activate the apoptotic cascade.[44,45]

A hallmark of apoptosis is the up-regulation of specific genes, whose proteins then carry out specific tasks or initiate subsequent molecular events that result in the death and removal of the cell.[46-48] Stigmata of apoptotic cell death include the formation of pyknotic

(electron-dense) nuclei, the precise internucleosomal cleavage of deoxyribonucleic acid, and the vesicular packaging of the cellular components into apoptotic bodies. Resident macrophages or surrounding cells with phagocytic capabilities then can remove the debris. Apoptosis does not usually involve an inflammatory response, and once a cell is removed by apoptosis, there may be little evidence that the cell was ever there in the first place.

The majority of the work on apoptosis in the eye has been in the study of the mechanisms of cell death in glaucoma and optic neuropathies.[49-57] Various experimental models of glaucoma and optic nerve injury have been developed, ranging from in vivo assays such as mechanical elevation of intraocular pressure or optic nerve crush, to in vitro work on growth and survival of cultured ganglion cells. All of these models show that the pathways for apoptosis play a major role in ganglion cell death and that interference with these pathways at various steps along the apoptotic cascade can enhance survival of these cells.

Apoptosis also appears to be the main mechanism of photoreceptor cell death in animal models of retinal degeneration.[58-60] The rate and amount of photoreceptor cell death in these models can be altered by modulating the apoptotic cascade by such means as the addition of trophic factors,[61-67] by modulation of the levels of apoptosis regulatory proteins,[68-71] and by glucocorticoid injections.[72] The role of caspase activation in photoreceptor cell death is controversial and may depend on the model used. Models in which photic injury is used to induce retinal degeneration may cause photoreceptor cell death via caspase-independent pathways.[73] Experiments in animal models that use a chemical induction of photoreceptor degeneration, however, suggest that caspase activation occurs and that caspase inhibitors can decrease the amount of cell death.[74,75] In the setting of retinal-RPE separation, however, the role of either excitotoxic amino acids or neurotrophic factors is poorly understood.

Detachment of the retina from the RPE results in significant levels of photoreceptor cell death.[76-78] The first insight into the molecular mechanisms that control photoreceptor death in the context of retinal-RPE separation was presented by Cook and coworkers in 1995.[25] Using the feline model of experimental retinal detachment, they showed that retinal detachment results in the formation of pyknotic nuclei, apoptotic bodies, and TUNEL-positive staining in the photoreceptor layer, suggesting activation of apoptosis pathways in the photoreceptors. At the same time, Chang and coworkers[79] presented similar histologic evidence that apoptosis was activated in the photoreceptors after traumatic retinal detachments in humans. Further work in a rabbit model of experimental retinal detachment also showed the presence of histologic markers of apoptosis in the photoreceptors.[80] Photoreceptors of detached retinas show a reorganization of their cytoskeleton consistent with apoptosis.[30] Retinal-RPE separation also increases the levels of excitotoxic amino acids in the microenvironment surrounding photoreceptors.[30] As stated before, supplemental oxygen can prevent some of the separation-induced photoreceptor death and glial cell changes, but the mechanisms responsible for this effect are unknown.[38]

Though it appeared that the detachment-induced death of photoreceptors occurs via apoptosis, very little was known about the specific molecular pathways that become activated by detachment and that regulate the death of the photoreceptors. The studies mentioned above presented histologic evidence of apoptosis activation but did not provide any details regarding the specific apoptosis pathways activated or the molecular control of these pathways.

In general, apoptosis is activated by one of 2 main pathways, the receptor-mediated pathway[81,82] and the intrinsic (mitochondrial) pathway.[83] A major activator of apoptosis is the fragment apoptosis stimulator (Fas) pathway. Fas, also referred to as CD95 or APO-1 (apoptosis-1) system, is a member of the tumor necrosis factor superfamily of genes and represents the prototypical member of this gene family. When the Fas ligand binds to the Fas receptor, it causes the sequential activation of various intermediary proteins that ultimately lead to the activation of caspase 3 and apoptotic cell death.

In contrast, activation of the intrinsic pathway does not require activation of a surface receptor, but rather results from the modification of intracellular pools of proteins. Intracellular stressors result in posttranslation modification of these proteins, which then exert their effect on the mitochondria to release cytochrome c. The released cytochrome c then binds with apoptosis activating factor-1 and caspase 9 to form a complex known as the apoptosome, which in turn activates more downstream apoptosis reactions. Fas-receptor activation, however, can also turn on the intrinsic pathway, usually through intermediary proteins such as Bid as well as other members of the Bcl-2 protein family. As with receptor-mediated apoptosis, the intrinsic pathway also converges on the effector caspases 3 and 7.

Using a rodent model of experimental retinal detachment, it was shown that the most downstream, convergent point in the apoptosis cascade, namely, caspase 3, caspase 7, and caspase 9, and poly-ADP ribose-polymerase were activated.[78] Looking more upstream in the apoptosis pathway, retinal-RPE separation was shown to result in the formation of the Fas-receptor/Fas-ligand complex and activation of caspase 8, the direct target of the bound (activated) Fas-receptor.[84] Injection of neutralizing antibodies against either the Fas receptor or the Fas ligand into the subretinal space resulted in the reduction of caspase 9 activity (a marker of intrinsic pathway activity) by approximately 50%.

The ability of an antibody against the Fas receptor to inhibit caspase 9 activity suggests a hierarchical linkage between the receptor-mediated and intrinsic apoptosis pathways. This linkage can be provided by the Fas-dependent activation of the protein Bid, a member of the Bcl-2 family of proapoptotic proteins and a target of activated caspase 8.[82] Retinal-RPE separation does, in fact, cause activation of Bid in the rodent model of retinal-RPE separation.[84] Taken together, these data suggest that formation of the Fas-receptor/Fas-ligand complex results in activation of caspase 8, which in turn activates Bid. The activation of Bid is known to stimulate, through the Bax protein, the release of cytochrome c from the mitochondria and activate the intrinsic pathway.[82] These findings are consistent with the results of Yang and coworkers,[85] who found decreased photoreceptor cell loss in a similar experimental model of retinal-RPE separation in a Bax-deficient mouse.

An important observation regarding the control of apoptosis was that retinal-RPE separation resulted in a marked increase in the transcription of the genes coding for proteins that are part of the Fas pathway.[84] It was first noted that there was a time-dependent

increase in the levels of Fas-receptor, Fas-ligand, caspase 8, Bid, and caspase 3 on Western blot analysis of protein extracts from separated retinas. Quantitative real-time polymerase chain reaction (qRT-PCR) was able to show that this was due, in part, to an increase in the level of the corresponding transcript. In contrast, the intrinsic pathway intermediates cytochrome c and caspase 9 had no significant changes in their transcript levels. This is consistent with the Western blot results, which did not reveal any time-dependent increase in the level of these two proteins. Immunostaining of the detached retina for caspase 3 showed increased protein staining in the outer nuclear layer, consistent with its role in photoreceptor apoptosis.[84]

Up-regulation of the Fas-receptor/Fas-ligand pathway has been well documented in experimental models of brain ischemia.[86-88] The intermediates of this pathway normally exist at very low levels, and the onset of expression occurs only after the injury.[88] Morphologically, the expression occurs most predominantly in the penumbral region of the ischemic injury, suggesting that receptor-mediated apoptosis plays a role in delayed cell death. In the case of retinal-RPE separation, photoreceptor cells that do not undergo immediate death have increased expression of receptor-mediated apoptosis pathway intermediates.[84] It is not clear why this occurs, but it may provide another mechanism to control and regulate the slow and cumulative loss of photoreceptor cells that occurs in chronic retinal detachments. This delayed apoptosis might occur independently of the intrinsic pathway, which has a peak activity at 24 hours after separation, and is not transcriptionally increased after the separation.[84]

The fact that there was an increase in the transcription of the Fas pathway genes after retinal-RPE separation suggested a novel point of intervention for preventing the detachment-induced death of the photoreceptor cells.[89] Reducing the detachment-induced increase in Fas-receptor transcript levels by injection of small inhibitory RNA against the Fas-receptor transcript prevented the detachment-induced increase in Fas-receptor messenger RNA (mRNA) and subsequent increase in Fas-receptor protein levels.[89] The effect of this reduced Fas-receptor activity was the increase in the number of photoreceptor cells that survived long periods of retinal-RPE separation. This effect was similar to preventing the activation of the Fas proapoptotic pathway at the protein level through the use of inhibitory antibodies that blocked the Fas-receptor, or when the retinal detachment was created in the LPR mouse strain that carries a gene that codes for a defective Fas-receptor.[89]

## SOME PHOTORECEPTORS SURVIVE RETINAL-RPE SEPARATION

An intriguing clinical observation that has been reproduced in animal models is that although retinal-RPE separation generally occurs at a discrete point in time, it does not induce an immediate death of all the photoreceptors, as might be expected when cells are removed from their nutritional and metabolic support. Although measurable decreases in outer nuclear layer thickness may occur in as little as 1 to 3 days after retinal-RPE separation, significant numbers of photoreceptors survive for many days, or even weeks.[77,78,90] Only if the retina remains separated from the RPE for a long enough period of time will the majority of photoreceptors die. This observation suggests that there are intrinsic antiapoptotic (ie, protective) pathways that become activated and that can maintain photoreceptor viability for a period of time. Such pathways have been described in a number of acute injury models in various tissues.[91-97] These pathways may regulate stress responses, metabolism, and cell-cell interaction. Given what is known about the time course of photoreceptor cell death after retinal-RPE separation, it seems highly probable that such antiapoptotic (ie, "prosurvival") pathways are also activated in the retina and that these pathways may play an important role in promoting photoreceptor cell survival after the trauma of retinal-RPE separation.

To begin to examine the question of whether "prosurvival" pathways are activated in the retina, a gene-microarray study was initiated to identify and define the changes in transcription that occur in the retina after separation from the RPE. The gene expression profile of retinas 24 hours after retinal-RPE separation was measured using the Affymetrix rat 230A GeneChip.[98] Using this technique, 27 genes were identified that exhibited a significant change in their expression in the separated vs the attached retinas. Among the genes detected on microarray, 3 (11%) correspond to the interleukin 6 (IL-6) prosurvival pathway. Additional functional clustering of the differentially expressed genes strongly suggested the increased transcription of genes belonging to the IL-6 pathway.

Members of the IL-6 cytokine family have been shown in multiple systems to prevent apoptosis. In multiple myeloma, IL-6 has a marked antiapoptotic effect.[99,100] Interleukin-6 has also been shown to have a very potent antiapoptotic effect in chemical models of hepatic cell injury.[101,102] In the hepatic injury model, this effect occurs, in part, by increasing the transcription of genes known to inhibit components of the Fas pathway.[103] The IL-6 cytokines exert their effect through the regulation of transcription.[104] Upon binding its receptor, IL-6 causes the phosphorylation of an intracellular molecule known as STAT (signal transducer and activator of transcription). The phosphorylated STAT then translocates from the cytoplasm to the nucleus to function as a transcription factor directly affecting gene expression. Other members of the IL-6 family work similarly through binding their respective receptors and activating members of the STAT family.

In neuronal systems, IL-6 enhances cell survival. In murine models of ischemic stroke, inhibition of IL-6 signaling results in increased cell death.[105] Similarly, in retinal ischemia/reperfusion injury, ganglion cell survival is enhanced by either increasing transcription of IL-6 by glial cells or adding exogenous IL-6.[106] Similarly, in a model of NMDA-mediated retinal ganglion cell injury, activation of the IL-6 system results in increased ganglion cell survival.[107] Ciliary neurotrophic growth factor (CNTF), also a member of the IL-6 family of cytokines, has been shown to be neuroprotective of photoreceptors in experimental models of hereditary retinal degeneration[66,67] and of retinal ganglion cells in models of optic nerve injury.[108,109]

Based upon the initial microarray data after 24 hours of retinal detachment, it was predicted that additional components of the IL-6 stress-response pathway would be transcriptionally altered at later time points.[98] Quantitative RT-PCR and immunoblot analysis on select components of this pathway were performed in retinas separated for 3 and 7 days. These confirmed the prediction, with significantly increased levels of transcript and protein for IL-6, as well as for STAT1 and STAT3. Interestingly, transcript and protein levels of CNTF were also found to be increased.

Upon binding to their respective receptors, both IL-6 and CNTF result in the phosphorylation and activation of STAT proteins. Separation-induced increases in the levels of phosphorylated STAT1 and phosphorylated-STAT3 were also detected,[110] consistent with activation of the IL-6/CNTF signaling pathway. These results were interpreted to mean that the retina, when separated from the RPE, induces the activation of intrinsic photoreceptor-protective pathways. This hypothesis was proven in an experimental model of retinal detachment, by using both loss- and gain-of-function experiments to show that IL-6 does, in fact, contribute significantly to photoreceptor survival during retinal detachment.[110]

### PRESENT STUDY: STATEMENT OF HYPOTHESIS

The previous sections outlined some of the significant changes that occur within the retina in response to separation from the RPE, including some examples of specific genes that undergo detachment-induced changes in their transcription levels. Little is known, however, about the overall transcriptional changes that occur within the retina that presumably trigger many of these detachment-induced changes, or how gene transcription levels in the retina change as a function of time after detachment. It is the basic hypothesis of this thesis that retinal-RPE separation results in a unique gene transcription profile within the retina. This hypothesis leads to the generation of 3 specific predictions. The first prediction is that significant differences will exist between the set of genes transcribed in the detached vs the attached retina. The second prediction is that this "gene transcription profile" changes as a function of time after detachment. The third prediction is that the genes being transcribed in the detached retina will belong to pathways known to regulate the types of morphologic and functional changes that occur in detached retinas. A corollary hypothesis states that the transcriptional changes detected above will be preceded by activation of one or more members of the mitogen-activated protein (MAP) kinase family of proteins, known stimulators of stress-response gene transcription. In this thesis, these hypotheses and predictions will be tested using a well-established rodent model of experimental retinal detachment. Gene transcript levels within the retina will be measured using gene microarray technology and validated using RT-PCR. Functional clustering of the altered gene profiles will be performed using computerized algorithms and correlated to the detachment-induced changes described above. Early activation (ie, phosphorylation) of MAP kinase proteins will be assessed using Western blot analysis.

## METHODS

### EXPERIMENTAL MODEL OF RETINAL-RPE SEPARATION

The experiments described in this study were performed using our rat model of experimental retinal-RPE separation that has been previously developed and validated.[78] In this model, a solution of 1% hyaluronic acid is injected into the subretinal space using a 32-gauge subretinal injector (Figure 1). This model is a simple and reproducible technique for creating experimental retinal-RPE separation that can persist for extended periods of time. This model has been used by multiple laboratories and is felt to mimic the morphologic and functional changes seen in human retinal detachments.

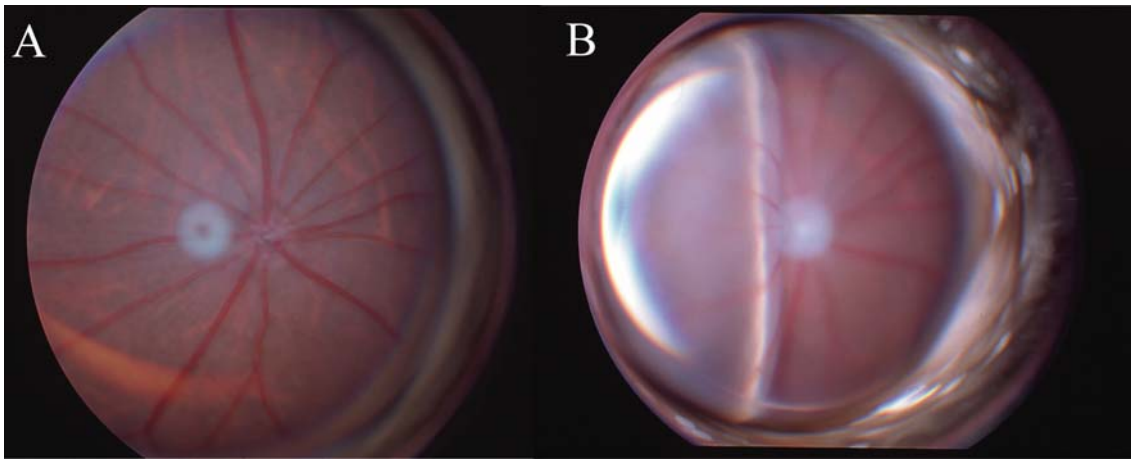


**FIGURE 1**

Experimental model of retinal–retinal pigment epithelial separation. A, Fundus photo of attached rat retina. (White halo to left of optic nerve is a photographic artifact.) B, Fundus photo of the rat retina where the nasal (left) half is detached with a subretinal injection of 1% hyaluronic acid. Typically one-third to one-half of the retina is detached.

All animal experiments were performed in accordance with the Association for Research in Vision and Ophthalmology Statement for the Use of Animals in Ophthalmic and Vision Research and the guidelines established by the University Committee on Use and Care of Animals of the University of Michigan. Retinal-RPE separations were created as previously described.[78] Briefly, adult Brown-Norway rats were anesthetized with a 50:50 mix of ketamine (100 mg/mL) and xylazine (20 mg/mL), and pupils were dilated with

topical phenylephrine (2.5%) and tropicamide (1%). A sclerotomy was created approximately 1 to 2 mm posterior to the limbus with a 20-gauge microvitreoretinal blade (Walcott Rx Products, Marmora, New Jersey), with special caution to avoid damaging the lens. A Glaser subretinal injector (32-gauge tip; BD Ophthalmic Systems, Sarasota, Florida) connected to a syringe filled with 10 mg/mL sodium hyaluronate (Healon; Pharmacia and Upjohn Co, Kalamazoo, Michigan) was introduced through the sclerotomy into the vitreous cavity. The tip of the subretinal injector was introduced into the subretinal space through a peripheral retinotomy, and the sodium hyaluronate was slowly injected, thus separating the neurosensory retina from the underlying RPE. In all experiments, approximately one-third to one-half of the retina becomes separated. Separation was performed in the left eye, with the right eye serving as the control. For control eyes, a sham surgery was performed in which all components of the procedure were carried out except introduction of the subretinal injector and elevation of the retina. In experimental eyes, only the separated portion of the retina was harvested for analysis.

## MICROARRAY AND STATISTICAL ANALYSIS

Microarray analysis was performed on retinas that were detached from the RPE for 3 periods of time: 1 day, 7 days, and 28 days. At each of these time points, the detached portion of the experimental eye's retina was harvested, as was the contralateral retina that received the sham treatment. For each time point, 8 animals were used. To obtain sufficient sample quantity to run on the gene microarray chip, retinas from 2 animals were pooled together. This resulted in 8 independent samples for each time point: 4 from detached eyes and 4 from attached eyes. Creation of the retinal detachment was timed such that all samples were harvested on the same day. This way, all samples could be processed together, so as to minimize the variability that could be introduced through operator handling.

To prepare the retinas for transcriptional analysis, we used a previously published protocol.[98] In brief, total RNA was extracted using Trizol (Invitrogen; Carlsbad, California) and purified using the RNeasy Mini Kit (Qiagen; Valencia, California). RNA quality was checked by gel electrophoresis. The first strand of complementary DNA (cDNA) was synthesized using 10 μg of total RNA, 1 μL of T7-(dT)24 primer (Invitrogen) (100 pmol/μL), and the Superscript II RNase H Reverse Transcriptase kit (Invitrogen), as per manufacturer's instructions. Second strand cDNA synthesis was performed by adding the single strand cDNA solution DEPC-H2O (91 μL), 5X second strand buffer (Invitrogen) (30 μL), 10 mM dNTP mix (Invitrogen) (3 μL), 10 U/μL *Escherichia coli* DNA ligase (Invitrogen) (1 μL), 10 U/μL *E coli* DNA polymerase I (Invitrogen) (4 μL), 2 U/μL *E coli* RNase H (Invitrogen) (1 μL), and incubated at 16°C for 2 hours. Then 2 μL of T4 DNA polymerase (Invitrogen) was added and the solution incubated at 16°C water bath for 5 minutes. The reaction was then stopped by adding 10 μL of 0.5M EDTA (Ambion; Austin, Texas). The double-stranded cDNA was purified using a prespin phase lock gel (PLG) tube (VWR Scientific; Chicago, Illinois) run for 30 seconds at 12,000× *g*. Phenol:chloroform:isoamyl alcohol (25:24:1) (Invitrogen) (162 μL) was added to the cDNA, vortexed briefly, and rerun through the PLG tubes for 2 minutes at 12,000× *g*. The aqueous phase was transferred to a fresh 1.5-mL tube and diluted 2:1 with 7.5 M NH4OAc (Sigma, St Louis, Missouri), and this mixture was diluted 1:2.5 with absolute ethanol. This mixture was vortexed thoroughly and centrifuged at room temperature for 20 minutes at 12,000× *g*. The pellet was washed twice with 0.5 mL of 80% ethanol. After air-drying, the dried pellet was resuspended in a RNase-free water and quantified by gel electrophoresis.

Biotin-labeled complementary RNA (cRNA) was synthesized using the BioArray High Yield RNA Transcript Labeling Kit (Enzo Life Sciences Inc, Farmingdale, New York) as per manufacturer's instructions. Product was purified and quantified as indicated above. Fragmentation of the cRNA was performed using the GeneChip Sample Cleanup Module Kit (Affymetrix Inc, Santa Clara, California). Fragmented cRNA was hybridized to the Affymetrix Rat 230A GeneChip (Affymetrix Inc) as per manufacturer's instructions. After hybridization, the chips were run through the Affymetrix fluidics station and scanned through the Affymetrix spectrophotometer (Affymetrix Inc). A total of 24 Affymetrix Rat 230A arrays were processed representing 4 detached samples and 4 attached samples at each of the 3 time points.

Affymetrix CEL files were used as the source for raw data values. Intensities were converted to log base 2 expression measures with the robust multi-array average (RMA) expression measure in the R Bioconductor Affy package.[111] The RMA method converts background-adjusted probe intensities to expression measures using the quantile normalization with corrections for optical noise and nonspecific binding factors.

Likely uninformative genes were excluded from statistical analysis when they had low variability. Genes whose expression differed by at least 1.5-fold from the median in at least 20% of the arrays were retained. Genes with more than 50% of data missing were also excluded. The filtering process resulted in 5,036 out of 15,923 probes included in the statistical analyses for all 3 time points, and 5,591 included in the comparison of days 1 to 7.

The "simpleaffy" function, "qc" (part of the Affymetrix Corporation software packet for microarray gene chip analysis) was used to generate commonly used quality control metrics. This function calculates values for average background, scale factor, number of genes called present (percent present), the 3′ to 5′ ratios for β-actin and glyceraldehyde 3-phosphate dehydrogenase (GAPDH), and spike-in control transcripts. These values are recognized criteria for determining whether the actual hybridization and scanning protocols were successful. Values were computed using the MAS 5.0 algorithm. Based on these criteria, 23 of the 24 microarrays we processed were deemed usable for further analysis. We had one microarray chip from the day 7 attached retina group that did not meet these quality control metrics and was excluded from all further analyses.

The normalization used by MAS 5.0 makes the assumption that gene expression does not change significantly for the vast majority of transcripts in an experiment. As a consequence, the trimmed mean intensity for each array should be constant, and, by default, MAS 5.0 scales the intensity for every sample so that each array has the same mean. The amount of scaling applied or scale factor provides

a measure of the overall expression level for an array and, assuming all else remains constant, a reflection of how much labeled RNA is hybridized to the chip. Large variations in scale factors denote instances that the normalization assumptions are likely to fail due to poor sample quality or an inappropriate amount of starting material. Alternatively, scale factor variations might occur if there have been problems with RNA extraction, labeling, scanning, or array manufacture. Affymetrix recommends that scale factors should be within a threefold range. None of our chips fell outside the threefold range.

The percent present call represents the fraction of probe sets called present on an array. Extremely low percent present values are a possible indication of poor sample quality. Three calls are made—present, marginal, and absent—by looking at the difference between perfect match (PM) and mismatch (MM) values for each probe pair in a probe set. Probe sets are flagged marginal or absent when the PM values for a probe set are not significantly above the MM values. As with scale factors, large or significant variations in percent present calls across different arrays in a study should be cautiously examined. Replicate samples should have similar percent present values. Our arrays have a percent present range from a low of 52.5 to a high of 67.8, values that are within the acceptable range.

Affymetrix designed probe sets to hybridize to either end of the long transcripts GAPDH and β-actin to assess RNA sample and assay quality. By comparing the signal from the 3′ probe set to either the mid or 5′ probe sets, a measure of the quality of the RNA hybridized to the chip is obtained. High ratios are an indication of the presence of truncated transcripts. The ratio of the 3′ probe set to the 5′ probe set should be less than 3. A high 3′ to 5′ ratio may indicate degraded RNA or inefficient transcription of double-stranded cDNA or biotinylated cRNA. GAPDH is a smaller gene than β-actin. As a consequence, its 3′ to 5′ ratio should always be at or around 1. The GAPDH 3′ to 5′ ratios for all but the excluded chip are within the recommended range. All of our chips showed acceptable β-actin values.

Analyses were performed using BRB-ArrayTools Version 3.6.0.[112] The random variance model was applied to the filtered data sets. This model assumes that the variance of the residuals in analysis of variance (ANOVA) for each gene is a random variable from a common inverse gamma distribution with unknown parameters. By sharing the variance estimate across multiple genes, one can form a better estimate for the true residual variance of a given gene and effectively boost the residual degrees of freedom.[113] Gene annotations were updated using the software package DAVID, available over the Internet (david.abcc.ncifcrf.gov). Average linkage Euclidean distance hierarchical clusters ("heatmaps") were generated with Cluster 3.0 and Java TreeView Version 1.1.1.[114,115]

## QUANTITATIVE REAL-TIME PCR VALIDATION OF GENE CHIP RESULTS

To help with validation of changes seen in transcript levels found on the microarray, we selected a subset of the genes found to have significantly altered transcript levels at 7 days postdetachment and measured the actual level of the transcript using qRT-PCR. For this experiment retinas detached for 7 days were obtained from animals different from those used in the microarray experiment, so as to have an independent sample for corroboration of any transcript level changes.

Real-time PCR was performed with the TaqMan Low Density Array (TLDA) microfluidic assay from Applied Biosystems Corporation. For this assay total RNA is isolated with Trizol reagent (Invitrogen). First strand cDNA synthesis was performed using 3 μg of total RNA, 200 units Superscript III reverse transcriptase (Invitrogen), and oligo$(dT)_{20}$ in a total reaction volume of 20 μL at 42°C for 2 hours. The reaction was terminated by heating. RNaseH was used to remove the template RNA. The reverse transcription products were diluted 1:4 in $dH_2O$. The TLDA assays were run as per manufacturer's instructions. Primers specific for the rat hypoxanthine phosphoribosyl transferase (rHPRT) gene were used as an internal control to allow for normalization and direct comparison between multiple samples. Primers were designed to span intron/exon boundaries to distinguish between transcripts and any contaminating genomic DNA. Samples lacking reverse transcriptase or cDNA template served as negative controls. For each gene, qRT-PCR was performed on samples derived from 3 different animals and repeated 3 times per animal. The average "-fold" change in expression relative to the rHPRT transcript level was then calculated.

## MAP KINASE PHOSPHORYLATION ASSAY: WESTERN BLOT ANALYSIS

MAP kinases typically exist in a proactive or inactive form in the cell cytoplasm. When an appropriate signal is received by the cell, a series of sequential transduction cascade reactions ultimately lead to the activation of the MAP kinase through the phosphorylation of the MAP kinase. The activated, or phosphorylated, MAP kinase has a different molecular weight from the inactive, or unphosphorylated MAP kinase, so the two can be differentiated on Western blots. We performed Western blots on retinas harvested from detached vs attached retinas and looked for the amount of phosphorylated vs nonphosphorylated MAP kinases. To confirm the detachment-specific activation of the MAP kinases, we performed these same experiments but in the presence of specific inhibitors of p42/p44 MAP kinase phosphorylation. Inhibition of MAP kinase phosphorylation was achieved with either subretinal injection of PD98059 (Promega, Madison, Wisconsin) or intraperitoneal injection of U0126 (Promega). Both compounds were delivered in a 1% solution of dimethyl sulfoxide (DMSO) in phosphate-buffered saline at a final concentration of 50 μM and 1 mM, respectively. The control group was treated with DMSO only. Western blot analyses were performed as previously described.[84] Briefly, retinas from experimental and control eyes were dissected from the RPE-choroid at specific time points after retinal detachment. Retinas were homogenized and lysed with buffer containing 10 mM HEPES (pH 7.6), 0.5% IGEPAL, 42 mM KCL, 1 mM PMSF, 1 mM EDTA, 1 mM EGTA, 1 mM DTT, 5 mM MgCL2, and 1 tablet of protease inhibitors per 10 mL buffer (Complete Mini; Roche Diagnostics GmbH, Mannheim, Germany). The homogenates were incubated on ice and centrifuged at 22,000 *g* at 4°C for 60 minutes. The protein concentration of the supernatant was determined using the Dc protein assay kit (Bio-Rad Laboratories; Hercules, California). The protein samples were loaded and run on SDS-polyacrylamide gels (4% to 20% Tris-HCL ready gels, Bio-Rad Laboratories). After electrophoretic separation the proteins were transferred onto polyvinylidene fluoride membranes (Immobilon-P). Membranes were placed in 5% nonfat powdered milk in TBS (150 mM NaCL, 50 mM Tris; pH 7.6) and incubated overnight at 4°C on a shaker.

Membranes were then incubated with the primary antibody in 2.5% powdered milk in TBS overnight at 40°C. Membranes were washed extensively with TBS-T (0.1%Tween 20) and then incubated with horseradish peroxidase–labeled secondary antibody (1:3000, Santa Cruz Biotechnology) for 1 hour at room temperature. Bands were visualized with ECL-Plus (Amersham, Piscataway, New Jersey) according to the manufacturer's instructions. Antibodies against the following proteins were used: p38 MAPK antibody (Cell Signaling Technology, Beverly, Massachusetts), phospho-p38 MAPK antibody (Cell Signaling Technology), p42/p44 MAPK antibody (Cell Signaling Technology), phosphor-p42/p44 antibody (Cell Signaling Technology), SAPK/JNK antibody (Cell Signaling Technology), and phosphor-SAPK/JNK antibody (Cell Signaling Technology). Equal loading was verified by Ponceau S staining and densitometry analysis of a nonspecific band present across all lanes.

## RESULTS

### MICROARRAY ANALYSIS

The underlying hypothesis of this thesis is that detachment of the retina from the RPE causes a significant change in the pattern of genes expressed within the cells of the retina. Four predictions were generated from this hypothesis, namely that (1) significant differences will exist between the set of genes transcribed in the detached vs the attached retina; (2) the gene transcription profile of the retina will change as a function of time after detachment; (3) the genes being transcribed in the detached retina will belong to pathways known to regulate the types of morphologic and functional changes that occur in detached retinas, and (4) activation of stress-response kinases, namely MAP kinase, occurs early after retinal-RPE separation. This thesis tested and confirmed the hypothesis and resulting predictions.

As predicted by the hypothesis, there are significant differences in the types of genes transcribed in detached vs attached retinas. Tables 1, 2, and 3 list the genes that differ in transcript levels between the detached and attached retinas for days 1, 7, and 28 postdetachment, respectively. At 1 day after retinal detachment, there are 44 genes with significantly altered transcript levels. This number increases markedly to 448 by day 7. Interestingly, this number drops back down to 47 by 28 days after retinal detachment. The analyses for these individual time points were performed using the ANOVA method described in the "Methods" section, with a false discovery rate (FDR) set at less than or equal to 0.1. The FDR is a mechanism for controlling the number of false positives.[116] In other words, a FDR of 0.1 means that there is a 10% chance that the gene listed as differentially expressed is not actually differentially expressed. For microarray analyses, FDR is the accepted mechanism for assigning significance to alterations in transcript levels, rather than *P* values alone. The statistical reasons for this are beyond the scope of this thesis, but the argument can be simplified to state that FDR takes into account the thousands of analyses (ie, genes being compared) on a gene chip and reduces the risk of introducing a multiple comparison error (ie, finding a difference to be significant only due to the fact that one is measuring multiple differences). We assigned the FDR level of 0.1 to allow for a more robust and inclusive level for detecting genes with differential transcription.

**TABLE 1. GENES FOUND TO HAVE SIGNIFICANTLY DIFFERENT TRANSCRIPT LEVELS AT ONE DAY POSTDETACHMENT USING A FALSE DISCOVERY RATE (FDR) OF ≤0.1 (LISTED ALPHABETICALLY)**

| GENE SYMBOL | GENE NAME | FDR |
|---|---|---|
| *Aatf* | apoptosis antagonizing transcription factor | 0.064 |
| *Ania4* | activity and neurotransmitter-induced early gene protein 4 (ania-4) | 0.02 |
| *Aqp1* | aquaporin 1 | 0.022 |
| *Arpc1b* | actin-related protein 2/3 complex, subunit 1B | 0.057 |
| *Asns* | asparagine synthetase | 0.004 |
| *Atf3* | activating transcription factor 3 | 0.001 |
| *Atf5* | activating transcription factor 5 | 0.031 |
| *Atp1a3* | ATPase, Na+/K+ transporting, alpha 3 polypeptide | 0.066 |
| *Atp1b2* | ATPase, Na+/K+ transporting, beta 2 polypeptide | 0.066 |
| *Car14* | carbonic anhydrase 14 | 0.003 |
| *Cars_predicted* | cysteinyl-tRNA synthetase (predicted) | 0.04 |
| *Cebpb* | CCAAT/enhancer binding protein (C/EBP), beta | 0.047 |
| *Cish* | cytokine inducible SH2-containing protein | 0.013 |
| *Cldn11* | claudin 11 | 0.012 |
| *Edn2* | endothelin 2 | 0.066 |
| *Eml2* | echinoderm microtubule associated protein like 2 | 0.004 |
| *Faim2* | Fas apoptotic inhibitory molecule 2 | 0.066 |

**TABLE 1 (CONTINUED). GENES FOUND TO HAVE SIGNIFICANTLY DIFFERENT TRANSCRIPT LEVELS AT ONE DAY POSTDETACHMENT USING A FALSE DISCOVERY RATE (FDR) OF ≤0.1 (LISTED ALPHABETICALLY)**

| GENE SYMBOL | GENE NAME | FDR |
|---|---|---|
| *Gfap* | glial fibrillary acidic protein | 0.016 |
| *Glul* | glutamate-ammonia ligase (glutamine synthetase) | 0.054 |
| *Hk2* | hexokinase 2 | 0.028 |
| *Hmox1* | heme oxygenase (decycling) 1 | 0.065 |
| *ISGF3G* | Interferon-dependent positive acting transcription factor 3 gamma | 0.004 |
| *Itfg3* | integrin alpha FG-GAP repeat containing 3 | 0.054 |
| *Itgb1* | integrin beta 1 (fibronectin receptor beta) | 0.033 |
| *Jun* | Jun oncogene | 0.054 |
| *Junb* | Jun-B oncogene | 0.022 |
| *Litaf* | LPS-induced TN factor | 0.039 |
| *Lnpep* | leucyl/cystinyl aminopeptidase | 0.066 |
| *Nfe2l2* | nuclear factor, erythroid derived 2, like 2 | 0.066 |
| *Opn1mw* | opsin 1 (cone pigments), medium-wave-sensitive (color blindness, deutan) | 0.082 |
| *Opn1sw* | opsin 1 (cone pigments), short-wave-sensitive (color blindness, tritan) | 0.013 |
| *Plekha8* | pleckstrin homology domain containing, family A (phosphoinositide-binding specific) member 8 | 0.039 |
| *Ppap2c* | phosphatidic acid phosphatase type 2c | 0.094 |
| *Ppp1r1b* | protein phosphatase 1, regulatory (inhibitor) subunit 1B | 0.004 |
| *Ripk1_predicted* | receptor (TNFRSF)-interacting serine-threonine kinase 1 (predicted) | 0.004 |
| *Sec16b* | SEC16 homolog B (S. cerevisiae) | 0.005 |
| *Slc24a1* | solute carrier family 24 (sodium/potassium/calcium exchanger), member 1 | 0.039 |
| *Slc25a30* | solute carrier family 25, member 30 | 0.017 |
| *Slc26a8_predicted* | solute carrier family 26, member 8 (predicted) | 0.003 |
| *Smarcd1_predicted* | SWI/SNF-related, matrix-associated, actin-dependent regulator of chromatin, subfamily d, member 1 (predicted) | 0.066 |
| *Stat1* | signal transducer and activator of transcription 1 | 0.064 |
| *Stat3* | signal transducer and activator of transcription 3 | 0.066 |
| *Tm4sf1_predicted* | transmembrane 4 superfamily member 1 (predicted) | 0.098 |
| *Trim25* | transcribed locus | 0.098 |

**TABLE 2. GENES FOUND TO HAVE SIGNIFICANTLY DIFFERENT TRANSCRIPT LEVELS AT SEVEN DAYS POSTDETACHMENT USING A FALSE DISCOVERY RATE (FDR) OF ≤0.1 (LISTED ALPHABETICALLY)**

| GENE SYMBOL | DESCRIPTION | FDR |
|---|---|---|
| *39700* | septin 9 | 0.025 |
| *A2m* | alpha-2 macroglobulin | 0.001 |
| *Acadl* | acyl-coenzyme A dehydrogenase, long-chain | 0.054 |
| *Acss2_predicted* | acyl-CoA synthetase short-chain family member 2 (predicted) | 0.033 |
| *Adamts1* | a disintegrin-like and metallopeptidase (reprolysin type) with thrombospondin type 1 motif, 1 | 0.003 |
| *Adfp* | adipose differentiation related protein | 0 |
| *Adrm1* | adhesion regulating molecule 1 | 0.054 |
| *Agtpbp1_predicted* | ATP/GTP binding protein 1 (predicted) | 0.089 |
| *Aif1* | allograft inflammatory factor 1 | 0 |

**TABLE 2 (CONTINUED). GENES FOUND TO HAVE SIGNIFICANTLY DIFFERENT TRANSCRIPT LEVELS AT SEVEN DAYS POSTDETACHMENT USING A FALSE DISCOVERY RATE (FDR) OF ≤0.1 (LISTED ALPHABETICALLY)**

| GENE SYMBOL | DESCRIPTION | FDR |
|---|---|---|
| *Akap12* | A kinase (PRKA) anchor protein (gravin) 12 | 0.093 |
| *Alpl* | alkaline phosphatase, liver/bone/kidney | 0.095 |
| *Ania4* | activity and neurotransmitter-induced early gene protein 4 (ania-4) | 0 |
| *Ankrd6* | ankyrin repeat domain 6 | 0.05 |
| *Anxa2* | annexin A2 | 0.054 |
| *Anxa3* | annexin A3 | 0 |
| *Anxa5* | annexin A5 | 0.013 |
| *Anxa7* | annexin A7 | 0.02 |
| *Apbb1ip* | amyloid beta (A4) precursor protein-binding, family B, member 1 interacting protein | 0.002 |
| *Apoe* | apolipoprotein E | 0.063 |
| *Aprt_predicted* | adenine phosphoribosyl transferase (predicted) | 0.068 |
| *Aqp1* | aquaporin 1 | 0.012 |
| *Arhgdib* | rho, GDP dissociation inhibitor (GDI) beta | 0.054 |
| *Arpc1b* | actin related protein 2/3 complex, subunit 1B | 0 |
| *Arpc4_predicted* | actin-related protein 2/3 complex, subunit 4 (predicted) | 0.094 |
| *Arr3* | arrestin 3, retinal | 0.018 |
| *Asahl_predicted* | N-acylsphingosine amidohydrolase (acid ceramidase)-like (predicted) | 0.07 |
| *Asns* | asparagine synthetase | 0.028 |
| *Ass1* | argininosuccinate synthetase 1 | 0.004 |
| *Atf3* | activating transcription factor 3 | 0 |
| *Atp1b2* | ATPase, Na+/K+ transporting, beta 2 polypeptide | 0.071 |
| *Atp2c1* | ATPase, Ca++-sequestering | 0.086 |
| *Axl /// LOC687188* | Axl receptor tyrosine kinase /// similar to AXL receptor tyrosine kinase | 0.001 |
| *B2m* | beta-2 microglobulin | 0.001 |
| *B4galt5_predicted* | UDP-Gal:betaGlcNAc beta 1,4-galactosyltransferase, polypeptide 5 (predicted) | 0.017 |
| *Birc4* | baculoviral IAP repeat-containing 4 | 0.096 |
| *Bst2* | bone marrow stromal cell antigen 2 | 0.036 |
| *C1qa* | complement component 1, q subcomponent, alpha polypeptide | 0 |
| *C1qb* | complement component 1, q subcomponent, beta polypeptide | 0 |
| *C1qc* | complement component 1, q subcomponent, C chain | 0 |
| *C1r* | complement component 1, r subcomponent | 0.044 |
| *C1s* | complement component 1, s subcomponent | 0 |
| *C3* | complement component 3 | 0 |
| *Capg* | capping protein (actin filament), gelsolin-like | 0.016 |
| *Car14* | carbonic anhydrase 14 | 0.033 |
| *Car3* | carbonic anhydrase 3 | 0.001 |
| *Carhsp1* | calcium regulated heat stable protein 1 | 0.001 |
| *Casc4_predicted* | cancer susceptibility candidate 4 (predicted) | 0.049 |
| *Casp3* | caspase 3, apoptosis-related cysteine protease | 0.012 |

**TABLE 2 (CONTINUED). GENES FOUND TO HAVE SIGNIFICANTLY DIFFERENT TRANSCRIPT LEVELS AT SEVEN DAYS POSTDETACHMENT USING A FALSE DISCOVERY RATE (FDR) OF ≤0.1 (LISTED ALPHABETICALLY)**

| GENE SYMBOL | DESCRIPTION | FDR |
|---|---|---|
| *Ccdc5* | coiled-coil domain containing 5 | 0.021 |
| *Ccl2* | chemokine (C-C motif) ligand 2 | 0 |
| *Ccnd1* | cyclin D1 | 0 |
| *Ccnd2* | cyclin D2 | 0.008 |
| *Cd151* | CD151 antigen (Raph blood group) | 0.063 |
| *Cd302* | CD302 antigen | 0.015 |
| *Cd44* | CD44 antigen | 0 |
| *Cd47* | CD47 antigen (Rh-related antigen, integrin-associated signal transducer) | 0.007 |
| *Cd48* | CD48 antigen | 0.005 |
| *Cd53* | CD53 antigen | 0 |
| *Cd63* | CD63 antigen | 0.018 |
| *Cd74* | CD74 antigen (invariant polypeptide of major histocompatibility complex, class II antigen-associated) | 0.001 |
| *Cd9* | CD9 antigen | 0.02 |
| *Cd99* | CD99 antigen | 0.08 |
| *Cdh13* | cadherin 13 | 0.046 |
| *Cdh2* | cadherin 2 | 0.096 |
| *Cdr2* | cerebellar degeneration-related 2 | 0.025 |
| *Cebpb* | CCAAT/enhancer binding protein (C/EBP), beta | 0.001 |
| *Centd2* | centaurin, delta 2 | 0.069 |
| *Cfh* | complement component factor H | 0.063 |
| *Cfp* | complement factor properdin | 0.087 |
| *Cgnl1* | cingulin-like 1 | 0.009 |
| *Cib1* | calcium and integrin binding 1 (calmyrin) | 0.029 |
| *Clic1* | chloride intracellular channel 1 | 0.003 |
| *Clu* | clusterin | 0.016 |
| *Cmtm6* | CKLF-like MARVEL transmembrane domain containing 6 | 0.023 |
| *Cngb1* | cyclic nucleotide gated channel beta 1 | 0.087 |
| *Cnp* | 2',3'-cyclic nucleotide 3' phosphodiesterase | 0.01 |
| *Cntf* | ciliary neurotrophic factor | 0.013 |
| *Coro1a* | coronin, actin binding protein 1A | 0 |
| *Cox4i2* | cytochrome c oxidase subunit IV isoform 2 | 0.021 |
| *Cp* | ceruloplasmin | 0.001 |
| *Cpne3_predicted* | copine III (predicted) | 0.06 |
| *Cpne8_predicted* | copine VIII (predicted) | 0.084 |
| *Cr1l* | complement component (3b/4b) receptor 1-like | 0.008 |
| *Crip2* | cysteine-rich protein 2 | 0.06 |
| *Crx* | cone-rod homeobox containing gene | 0.095 |
| *Cryaa* | crystallin, alpha A | 0.009 |
| *Cryba1* | crystallin, beta A1 | 0.015 |
| *Cryba2* | crystallin, beta A2 | 0.02 |
| *Cryba4* | crystallin, beta A4 | 0.095 |
| *Crybb2* | crystallin, beta B2 | 0.065 |
| *Crybb3* | crystallin, beta B3 | 0.041 |

**TABLE 2 (CONTINUED). GENES FOUND TO HAVE SIGNIFICANTLY DIFFERENT TRANSCRIPT LEVELS AT SEVEN DAYS POSTDETACHMENT USING A FALSE DISCOVERY RATE (FDR) OF ≤0.1 (LISTED ALPHABETICALLY)**

| GENE SYMBOL | DESCRIPTION | FDR |
|---|---|---|
| *Crygs_predicted /// LOC681467* | similar to beta crystallin S (gamma crystallin S) /// crystallin, gamma S (predicted) | 0.013 |
| *Csf1r* | colony stimulating factor 1 receptor | 0.001 |
| *Csrp1* | cysteine and glycine-rich protein 1 | 0.021 |
| *Ctnna1* | catenin (cadherin associated protein), alpha 1 | 0.087 |
| *Ctsc* | cathepsin C | 0.001 |
| *Ctsh* | cathepsin H | 0.011 |
| *Ctss* | cathepsin S | 0.021 |
| *Ctsz* | cathepsin Z | 0 |
| *Cxcl13* | chemokine (C-X-C motif) ligand 13 | 0 |
| *Cxcl16* | chemokine (C-X-C motif) ligand 16 | 0.009 |
| *Cyba* | cytochrome b-245, alpha polypeptide | 0.002 |
| *Dag1* | dystroglycan 1 | 0.085 |
| *Dap* | death-associated protein | 0.001 |
| *Dcakd* | dephospho-CoA kinase domain containing | 0.073 |
| *Dtx3l* | deltex 3-like (Drosophila) | 0 |
| *Dusp1* | dual specificity phosphatase 1 | 0.098 |
| *Dusp6* | dual specificity phosphatase 6 | 0.031 |
| *Dyrk2_predicted* | dual-specificity tyrosine-(Y)-phosphorylation regulated kinase 2 (predicted) | 0.085 |
| *Edn2* | endothelin 2 | 0.004 |
| *Ednrb* | endothelin receptor type B | 0.035 |
| *Eef1d* | eukaryotic translation elongation factor 1 delta (guanine nucleotide exchange protein) | 0.086 |
| *Egfr* | epidermal growth factor receptor | 0.01 |
| *Eif2ak2* | eukaryotic translation initiation factor 2-alpha kinase 2 | 0.052 |
| *Elk3_predicted* | ELK3, member of ETS oncogene family (predicted) | 0 |
| *Enpp2* | ectonucleotide pyrophosphatase/phosphodiesterase 2 | 0.016 |
| *Ets2* | E26 avian leukemia oncogene 2, 3' domain | 0.054 |
| *Evi2a /// LOC688044* | ecotropic viral integration site 2A /// similar to ecotropic viral integration site 2A | 0.053 |
| *Exoc5* | exocyst complex component 5 | 0.018 |
| *Exoc6* | exocyst complex component 6 | 0.004 |
| *F2r* | coagulation factor II (thrombin) receptor | 0.054 |
| *F5* | coagulation factor V | 0.014 |
| *Faim2* | Fas apoptotic inhibitory molecule 2 | 0.095 |
| *Fam84a* | family with sequence similarity 84, member A | 0.004 |
| *Fbn1* | fibrillin 1 | 0.093 |
| *Fbxl6* | F-box and leucine-rich repeat protein 6 | 0.042 |
| *Fcer1a* | Fc receptor, IgE, high affinity I, alpha polypeptide | 0.087 |
| *Fcgr2b* | Fc receptor, IgG, low affinity IIb | 0.002 |
| *Fcgr3a* | Fc fragment of IgG, low affinity IIIa, receptor | 0 |
| *Fhl1* | four and a half LIM domains 1 | 0.073 |
| *Flna_predicted* | filamin, alpha (predicted) | 0.013 |
| *Flot2* | flotillin 2 | 0.03 |

**TABLE 2 (CONTINUED). GENES FOUND TO HAVE SIGNIFICANTLY DIFFERENT TRANSCRIPT LEVELS AT SEVEN DAYS POSTDETACHMENT USING A FALSE DISCOVERY RATE (FDR) OF ≤0.1 (LISTED ALPHABETICALLY)**

| GENE SYMBOL | DESCRIPTION | FDR |
|---|---|---|
| *Fmod* | fibromodulin | 0.041 |
| *Fn1* | fibronectin 1 | 0.02 |
| *Frmd8* | FERM domain containing 8 | 0.046 |
| *Ftl1* | ferritin light chain 1 | 0.014 |
| *Fxyd3* | FXYD domain-containing ion transport regulator 3 | 0.001 |
| *Gad1* | glutamic acid decarboxylase 1 | 0.089 |
| *Gadd45g* | growth arrest and DNA-damage-inducible 45 gamma | 0.004 |
| *Gal* | galanin | 0 |
| *Gamt* | guanidinoacetate methyltransferase | 0.028 |
| *Gatm* | glycine amidinotransferase (L-arginine:glycine amidinotransferase) | 0.058 |
| *Gbp2* | guanylate nucleotide binding protein 2 | 0 |
| *Gfap* | glial fibrillary acidic protein | 0 |
| *Gja1* | gap junction protein, alpha 1 | 0.036 |
| *Gldc_predicted* | glycine decarboxylase (predicted) | 0.013 |
| *Gltp_predicted* | glycolipid transfer protein (predicted) | 0.001 |
| *Gmfg* | glia maturation factor, gamma | 0.065 |
| *Gnai3* | guanine nucleotide binding protein, alpha inhibiting 3 | 0.065 |
| *Gnb1* | guanine nucleotide binding protein, beta 1 | 0.037 |
| *Gnb2* | guanine nucleotide binding protein, beta 2 | 0.033 |
| *Gnb3* | guanine nucleotide binding protein, beta 3 | 0.006 |
| *Gpm6b* | glycoprotein m6b | 0.007 |
| *Gpnmb* | glycoprotein (transmembrane) nmb | 0 |
| *Gpr56* | G protein-coupled receptor 56 | 0.037 |
| *Gpr61_predicted* | G protein-coupled receptor 61 (predicted) | 0.087 |
| *Gpx1* | glutathione peroxidase 1 | 0.001 |
| *Grk1* | G protein-coupled receptor kinase 1 | 0.041 |
| *Grn* | granulin | 0.001 |
| *Gsto1* | glutathione S-transferase omega 1 | 0.078 |
| *Gstt1 /// Gstt3* | glutathione S-transferase theta 1 /// glutathione S-transferase, theta 3 | 0.003 |
| *Hadh* | hydroxyacyl-coenzyme A dehydrogenase | 0.053 |
| *Hexb* | hexosaminidase B | 0.097 |
| *Hk2* | hexokinase 2 | 0.006 |
| *Hla-dma* | major histocompatibility complex, class II, DM alpha | 0.001 |
| *Hla-dmb* | major histocompatibility complex, class II, DM beta | 0.008 |
| *Hn1l* | hematological and neurological expressed 1-like | 0.028 |
| *Homer1* | homer homolog 1 (Drosophila) | 0.013 |
| *Hsd17b10* | hydroxysteroid (17-beta) dehydrogenase 10 | 0.089 |
| *Hsd17b4* | hydroxysteroid (17-beta) dehydrogenase 4 | 0.087 |
| *Hspb1* | heat shock protein 1 | 0.001 |
| *Htr1f* | 5-hydroxytryptamine (serotonin) receptor 1F | 0.056 |
| *Icam1* | intercellular adhesion molecule 1 | 0 |
| *Id3* | inhibitor of DNA binding 3 | 0.09 |
| *Ifi27l* | interferon, alpha-inducible protein 27-like | 0.001 |

**TABLE 2 (CONTINUED). GENES FOUND TO HAVE SIGNIFICANTLY DIFFERENT TRANSCRIPT LEVELS AT SEVEN DAYS POSTDETACHMENT USING A FALSE DISCOVERY RATE (FDR) OF ≤0.1 (LISTED ALPHABETICALLY)**

| GENE SYMBOL | DESCRIPTION | FDR |
|---|---|---|
| *Ifi30* | interferon gamma inducible protein 30 | 0.001 |
| *Ifitm1_predicted* | interferon induced transmembrane protein 1 (predicted) | 0 |
| *Ifitm2* | interferon induced transmembrane protein 2 | 0 |
| *Ifitm3* | interferon induced transmembrane protein 3 | 0.001 |
| *Ifngr1* | interferon gamma receptor 1 | 0.003 |
| *Ifngr2_predicted* | interferon gamma receptor 2 (predicted) | 0.044 |
| *Ihpk2* | inositol hexaphosphate kinase 2 | 0.025 |
| *Il13ra1* | interleukin 13 receptor, alpha 1 | 0.07 |
| *Impg1* | interphotoreceptor matrix proteoglycan 1 | 0.03 |
| *Iqwd1* | IQ motif and WD repeats 1 | 0.09 |
| *Irf1* | interferon regulatory factor 1 | 0 |
| *Irf7* | interferon regulatory factor 7 | 0.011 |
| *Itfg3* | integrin alpha FG-GAP repeat containing 3 | 0.003 |
| *Itgb1* | integrin beta 1 (fibronectin receptor beta) | 0.004 |
| *Itgb1* | integrin beta 1 (fibronectin receptor beta) | 0.033 |
| *Jak3* | Janus kinase 3 | 0.033 |
| *Jun* | Jun oncogene | 0.012 |
| *Junb* | Jun-B oncogene | 0.015 |
| *Klf10* | Kruppel-like factor 10 | 0.005 |
| *Klf6* | Kruppel-like factor 6 | 0.052 |
| *L3mbtl3_predicted* | l(3)mbt-like 3 (Drosophila) (predicted) | 0.054 |
| *Lad1_predicted* | ladinin (predicted) | 0.001 |
| *Lamb2* | laminin, beta 2 | 0.06 |
| *Lamp2* | lysosomal membrane glycoprotein 2 | 0.095 |
| *Lap3* | leucine aminopeptidase 3 | 0.064 |
| *Laptm5* | lysosomal-associated protein transmembrane 5 | 0 |
| *Lcn2* | lipocalin 2 | 0 |
| *Lcp1* | lymphocyte cytosolic protein 1 | 0.004 |
| *Leprel2_predicted* | leprecan-like 2 (predicted) | 0.05 |
| *Lgals1* | lectin, galactose binding, soluble 1 | 0.084 |
| *Lgals3* | lectin, galactose binding, soluble 3 | 0 |
| *Lgals3bp* | lectin, galactoside-binding, soluble, 3 binding protein | 0 |
| *Lgi2_predicted* | leucine-rich repeat LGI family, member 2 (predicted) | 0.001 |
| *Lhfpl2_predicted* | lipoma HMGIC fusion partner-like 2 (predicted) | 0.022 |
| *Lipa* | lysosomal acid lipase A | 0.068 |
| *Litaf* | LPS-induced TN factor | 0 |
| *Lmbr1l* | limb region 1-like homolog (mouse) | 0.064 |
| *LOC498957* | similar to cDNA sequence BC025816 | 0.034 |
| *LOC499749* | similar to RIKEN cDNA C430004E15 | 0.045 |
| *LOC679295* | similar to dedicator of cytokinesis protein 1 (180 kDa protein downstream of CRK) (DOCK180) | 0.068 |
| *LOC680692 /// LOC682869* | similar to Golgi phosphoprotein 2 (Golgi membrane protein GP73) | 0.017 |
| *LOC680835* | similar to cullin 7 | 0.043 |
| *LOC686701* | similar to protein KIAA1404 | 0.014 |

**TABLE 2 (CONTINUED). GENES FOUND TO HAVE SIGNIFICANTLY DIFFERENT TRANSCRIPT LEVELS AT SEVEN DAYS POSTDETACHMENT USING A FALSE DISCOVERY RATE (FDR) OF ≤0.1 (LISTED ALPHABETICALLY)**

| GENE SYMBOL | DESCRIPTION | FDR |
|---|---|---|
| *LOC690349* | hypothetical protein LOC690349 | 0.038 |
| *Lrrc15* | leucine rich repeat containing 15 | 0.081 |
| *Lrrc46* | leucine rich repeat containing 46 | 0.089 |
| *Ltbr* | lymphotoxin B receptor | 0.068 |
| *Ly86_predicted* | lymphocyte antigen 86 (predicted) | 0.062 |
| *Lyz* | lysozyme | 0 |
| *Mak10* | MAK10 homolog, amino-acid N-acetyltransferase subunit, (S. cerevisiae) | 0.013 |
| *Mamdc2* | MAM domain containing 2 | 0.01 |
| *Map3k12* | mitogen activated protein kinase kinase kinase 12 | 0.068 |
| *Matn2_predicted* | matrilin 2 (predicted) | 0.005 |
| *MGC108823* | similar to interferon-inducible GTPase | 0.023 |
| *MGC125239* | hypothetical protein LOC686179 | 0.053 |
| *MGC94600* | scotin | 0.017 |
| *Mgp* | matrix Gla protein | 0.004 |
| *Mgst1* | microsomal glutathione S-transferase 1 | 0.021 |
| *Miox* | myo-inositol oxygenase | 0.02 |
| *Mmp14* | matrix metallopeptidase 14 (membrane-inserted) | 0.052 |
| *Msrb2* | methionine sulfoxide reductase B2 | 0.033 |
| *Mt1a* | metallothionein 1a | 0.038 |
| *Mt2A* | metallothionein 2A | 0.003 |
| *Mvp* | major vault protein | 0.001 |
| *Mx2* | myxovirus (influenza virus) resistance 2 | 0.086 |
| *Myh6* | myosin, heavy polypeptide 6, cardiac muscle, alpha | 0.052 |
| *Myh9* | myosin, heavy polypeptide 9, non-muscle | 0.08 |
| *Nadk* | NAD kinase | 0.061 |
| *Naprt1* | nicotinate phosphoribosyltransferase domain containing 1 | 0.014 |
| *Necap2* | NECAP endocytosis associated 2 | 0.07 |
| *Nek6* | NIMA (never in mitosis gene a)-related expressed kinase 6 | 0.018 |
| *Nfe2l2* | nuclear factor, erythroid derived 2, like 2 | 0.036 |
| *Nfib* | nuclear factor I/B | 0.083 |
| *Nfkb1* | nuclear factor of kappa light polypeptide gene enhancer in B-cells 1, p105 | 0.068 |
| *Nfyb* | nuclear transcription factor-Y beta | 0.045 |
| *Nlrp6* | NLR family, pyrin domain containing 6 | 0.004 |
| *Nme2* | expressed in non-metastatic cells 2 | 0.03 |
| *Nnat* | neuronatin | 0.066 |
| *Nnt* | nicotinamide nucleotide transhydrogenase | 0.044 |
| *Notch1* | Notch gene homolog 1 (Drosophila) | 0.003 |
| *Notch2* | Notch gene homolog 2 (Drosophila) | 0.023 |
| *Np* | nucleoside phosphorylase | 0.019 |
| *Npc2* | Niemann Pick type C2 | 0.053 |
| *Nrp1* | neuropilin 1 | 0.093 |
| *Nt5e* | 5' nucleotidase, ecto | 0.096 |
| *Nxn_predicted* | nucleoredoxin (predicted) | 0.07 |

**TABLE 2 (CONTINUED). GENES FOUND TO HAVE SIGNIFICANTLY DIFFERENT TRANSCRIPT LEVELS AT SEVEN DAYS POSTDETACHMENT USING A FALSE DISCOVERY RATE (FDR) OF ≤0.1 (LISTED ALPHABETICALLY)**

| GENE SYMBOL | DESCRIPTION | FDR |
|---|---|---|
| *Oaf* | OAF homolog (Drosophila) | 0.034 |
| *Odz2* | odd Oz/ten-m homolog 2 (Drosophila) | 0.091 |
| *Ogn* | osteoglycin | 0.044 |
| *Olfml3_predicted* | olfactomedin-like 3 (predicted) | 0.02 |
| *Opn1mw* | opsin 1 (cone pigments), medium-wave-sensitive (color blindness, deutan) | 0.007 |
| *Opn1sw* | opsin 1 (cone pigments), short-wave-sensitive (color blindness, tritan) | 0.045 |
| *Optn* | optineurin | 0.037 |
| *Ostf1* | osteoclast stimulating factor 1 | 0.07 |
| *Pacsin2* | protein kinase C and casein kinase substrate in neurons 2 | 0.051 |
| *Parp9_predicted* | poly (ADP-ribose) polymerase family, member 9 (predicted) | 0.053 |
| *Pax4* | paired box gene 4 | 0.033 |
| *Pcsk2* | proprotein convertase subtilisin/kexin type 2 | 0.002 |
| *Pdpn* | podoplanin | 0 |
| *Pfkfb2* | 6-phosphofructo-2-kinase/fructose-2,6-biphosphatase 2 | 0.095 |
| *Pgs1* | phosphatidylglycerophosphate synthase 1 | 0.085 |
| *Pla2g4a* | phospholipase A2, group IVA (cytosolic, calcium-dependent) | 0.009 |
| *Pla2g5* | phospholipase A2, group V | 0.086 |
| *Plac8_predicted* | placenta-specific 8 (predicted) | 0 |
| *Plagl2_predicted* | pleiomorphic adenoma gene-like 2 (predicted) | 0.1 |
| *Plat* | plasminogen activator, tissue | 0.004 |
| *Pld4* | phospholipase D family, member 4 | 0.001 |
| *Plekha8* | pleckstrin homology domain containing, family A (phosphoinositide binding specific) member 8 | 0.05 |
| *Pold4* | polymerase (DNA-directed), delta 4 | 0.008 |
| *Polg2_predicted* | polymerase (DNA directed), gamma 2, accessory subunit (predicted) | 0.054 |
| *Postn_predicted* | periostin, osteoblast specific factor (predicted) | 0 |
| *Ppap2a* | phosphatidic acid phosphatase 2a | 0.016 |
| *Ppap2b* | phosphatidic acid phosphatase type 2B | 0.035 |
| *Ppap2c* | phosphatidic acid phosphatase type 2c | 0.043 |
| *Ppargc1a* | peroxisome proliferative activated receptor, gamma, coactivator 1 alpha | 0.099 |
| *Ppp1r14b* | protein phosphatase 1, regulatory (inhibitor) subunit 14B | 0.01 |
| *Ppp1r1b* | protein phosphatase 1, regulatory (inhibitor) subunit 1B | 0.045 |
| *Ppp3cc* | protein phosphatase 3, catalytic subunit, gamma isoform | 0.077 |
| *Prdm1_predicted* | PR domain containing 1, with ZNF domain (predicted) | 0.079 |
| *Prkcdbp* | protein kinase C, delta binding protein | 0.085 |
| *Pros1* | protein S (alpha) | 0.048 |
| *Prss23* | protease, serine, 23 | 0.068 |

**TABLE 2 (CONTINUED). GENES FOUND TO HAVE SIGNIFICANTLY DIFFERENT TRANSCRIPT LEVELS AT SEVEN DAYS POSTDETACHMENT USING A FALSE DISCOVERY RATE (FDR) OF ≤0.1 (LISTED ALPHABETICALLY)**

| GENE SYMBOL | DESCRIPTION | FDR |
|---|---|---|
| *Psmb8* | proteasome (prosome, macropain) subunit, beta type 8 (large multifunctional peptidase 7) | 0 |
| *Psme1* | proteasome (prosome, macropain) 28 subunit, alpha | 0.008 |
| *Psme2* | proteasome (prosome, macropain) 28 subunit, beta | 0.025 |
| *Ptn* | pleiotrophin | 0.073 |
| *Ptprc* | protein tyrosine phosphatase, receptor type, C | 0.006 |
| *Ptprg* | protein tyrosine phosphatase, receptor type, G | 0.095 |
| *Ptprn2* | protein tyrosine phosphatase, receptor type, N polypeptide 2 | 0.022 |
| *Rab31* | RAB31, member RAS oncogene family | 0.086 |
| *Rab34* | RAB34, member of RAS oncogene family | 0.055 |
| *Rab3a* | RAB3A, member RAS oncogene family | 0.077 |
| *Rab3b* | RAB3B, member RAS oncogene family | 0.068 |
| *Rac2* | RAS-related C3 botulinum substrate 2 | 0.063 |
| *Raly* | hnRNP-associated with lethal yellow | 0.017 |
| *Rarres2* | retinoic acid receptor responder (tazarotene induced) 2 | 0.01 |
| *Rassf4* | Ras association (RalGDS/AF-6) domain family 4 | 0.008 |
| *Rbp1* | retinol binding protein 1, cellular | 0.027 |
| *Rcn1_predicted* | reticulocalbin 1 (predicted) | 0.054 |
| *Rdh10* | retinol dehydrogenase 10 (all-trans) | 0.034 |
| *Rdh11* | retinol dehydrogenase 11 | 0.082 |
| *RGD1303130* | kidney predominant protein NCU-G1 | 0.064 |
| *RGD1304579* | similar to 9230105E10Rik protein | 0.009 |
| *RGD1305793* | similar to hypothetical protein FLJ20154 | 0.017 |
| *RGD1306534_predicted* | similar to P-Rex1 (predicted) | 0.025 |
| *RGD1306959_predicted* | similar to C11orf17 protein (predicted) | 0.017 |
| *RGD1306959_predicted* | similar to C11orf17 protein (predicted) | 0.051 |
| *RGD1307801* | similar to RIKEN cDNA 1300018I05 | 0.05 |
| *RGD1308116_predicted* | similar to hypothetical protein MGC42105 (predicted) | 0.064 |
| *RGD1309105_predicted* | Similar to RIKEN cDNA 2310005N03 gene | 0.091 |
| *RGD1310799_predicted* | similar to RIKEN cDNA A930008G19 (predicted) | 0.094 |
| *RGD1311122* | similar to RIKEN cDNA 1110003E01 | 0.072 |
| *RGD1560601_predicted* | similar to Jumonji/ARID domain-containing protein 1C (SmcX protein) (predicted) | 0.089 |
| *RGD1561455_predicted* | similar to Ras GTPase-activating-like protein IQGAP2 (predicted) | 0.057 |
| *RGD1562952_predicted* | similar to Erbb2 interacting protein isoform 2 (predicted) | 0.065 |
| *RGD1563091_predicted* | similar to OEF2 (predicted) | 0.054 |
| *RGD1565557_predicted* | similar to RIKEN cDNA 2010301N04 (predicted) | 0.085 |
| *RGD1566215_predicted* | similar to coatomer gamma-2 subunit (gamma-2 coat protein) (gamma-2 COP) (predicted) | 0.001 |
| *RGD1566254_predicted* | RGD1566254 (predicted) | 0 |
| *RGD1566401_predicted* | Similar to GTL2, imprinted maternally expressed untranslated (predicted) | 0.054 |
| *Rgr_predicted* | retinal G protein coupled receptor (predicted) | 0.044 |

**TABLE 2 (CONTINUED). GENES FOUND TO HAVE SIGNIFICANTLY DIFFERENT TRANSCRIPT LEVELS AT SEVEN DAYS POSTDETACHMENT USING A FALSE DISCOVERY RATE (FDR) OF ≤0.1 (LISTED ALPHABETICALLY)**

| GENE SYMBOL | DESCRIPTION | FDR |
|---|---|---|
| *Rgs10* | regulator of G-protein signalling 10 | 0.003 |
| *Ril* | reversion induced LIM gene | 0 |
| *Ripk1_predicted* | receptor (TNFRSF)-interacting serine-threonine kinase 1 (predicted) | 0.036 |
| *Rnaset2_predicted* | ribonuclease T2 (predicted) | 0.009 |
| *Rpe65* | retinal pigment epithelium 65 | 0.005 |
| *Rpgrip1* | retinitis pigmentosa GTPase regulator interacting protein 1 | 0.026 |
| *Rrp1b* | ribosomal RNA processing 1 homolog B (S. cerevisiae) | 0.09 |
| *Rsad2* | radical S-adenosyl methionine domain containing 2 | 0.001 |
| *RT1-Aw2* | RT1 class Ib, locus Aw2 | 0.028 |
| *S100a10* | S100 calcium binding protein A10 (calpactin) | 0.065 |
| *S100a16_predicted* | S100 calcium binding protein A16 (predicted) | 0.073 |
| *S100a3* | S100 calcium binding protein A3 | 0 |
| *S100a4* | S100 calcium-binding protein A4 | 0 |
| *S100a6* | S100 calcium binding protein A6 (calcyclin) | 0.007 |
| *Sat1* | spermidine/spermine N1-acetyl transferase 1 | 0.08 |
| *Scarb2* | scavenger receptor class B, member 2 | 0.052 |
| *Scg2* | secretogranin II | 0.073 |
| *Sema5a_predicted* | sema domain, seven thrombospondin repeats (type 1 and type 1-like), transmembrane domain (TM) and short cytoplasmic domain, (semaphorin) 5A (predicted) | 0.046 |
| *Serpina3n* | serine (or cysteine) peptidase inhibitor, clade A, member 3N | 0 |
| *Serpinb1a* | serine (or cysteine) proteinase inhibitor, clade B, member 1a | 0.001 |
| *Serping1* | serine (or cysteine) peptidase inhibitor, clade G, member 1 | 0 |
| *Serpinh1* | serine (or cysteine) peptidase inhibitor, clade H, member 1 | 0.066 |
| *Sfrs2ip* | splicing factor, arginine/serine-rich 2, interacting protein | 0.068 |
| *Sh2b3* | SH2B adaptor protein 3 | 0.061 |
| *Sh3bgrl3_predicted* | SH3 domain binding glutamic acid-rich protein-like 3 (predicted) | 0.043 |
| *Sh3gl2* | SH3-domain GRB2-like 2 | 0.071 |
| *Slc11a2* | solute carrier family 11 (proton-coupled divalent metal ion transporters), member 2 | 0.08 |
| *Slc15a2* | solute carrier family 15 (H+/peptide transporter), member 2 | 0.086 |
| *Slc17a7* | solute carrier family 17 (sodium-dependent inorganic phosphate cotransporter), member 7 | 0.003 |
| *Slc1a2* | solute carrier family 1 (glial high affinity glutamate transporter), member 2 | 0.081 |
| *Slc1a3* | solute carrier family 1 (glial high affinity glutamate transporter), member 3 | 0.051 |
| *Slc20a2* | solute carrier family 20, member 2 | 0.044 |

**TABLE 2 (CONTINUED). GENES FOUND TO HAVE SIGNIFICANTLY DIFFERENT TRANSCRIPT LEVELS AT SEVEN DAYS POSTDETACHMENT USING A FALSE DISCOVERY RATE (FDR) OF ≤0.1 (LISTED ALPHABETICALLY)**

| GENE SYMBOL | DESCRIPTION | FDR |
|---|---|---|
| *Slc22a15_predicted* | solute carrier family 22 (organic cation transporter), member 15 (predicted) | 0.07 |
| *Slc24a1* | solute carrier family 24 (sodium/potassium/calcium exchanger), member 1 | 0.041 |
| *Slc25a29* | solute carrier family 25 (mitochondrial carrier, palmitoylcarnitine transporter), member 29 | 0.07 |
| *Slc25a30* | solute carrier family 25, member 30 | 0.001 |
| *Slc26a8_predicted* | solute carrier family 26, member 8 (predicted) | 0 |
| *Slc3a1* | solute carrier family 3, member 1 | 0.048 |
| *Slc4a7* | solute carrier family 4, sodium bicarbonate cotransporter, member 7 | 0.024 |
| *Slc6a6* | solute carrier family 6 (neurotransmitter transporter, taurine), member 6 | 0.018 |
| *Slc7a1* | solute carrier family 7 (cationic amino acid transporter, y+ system), member 1 | 0.087 |
| *Slco1a4* | solute carrier organic anion transporter family, member 1a4 | 0.089 |
| *Smarcd1_predicted* | SWI/SNF related, matrix associated, actin dependent regulator of chromatin, subfamily d, member 1 (predicted) | 0.054 |
| *Smarcd3* | SWI/SNF related, matrix associated, actin dependent regulator of chromatin, subfamily d, member 3 | 0.058 |
| *Smpdl3a* | sphingomyelin phosphodiesterase, acid-like 3A | 0.058 |
| *Sp110* | SP110 nuclear body protein | 0.001 |
| *Sparc* | secreted acidic cysteine rich glycoprotein | 0.027 |
| *Spp1* | secreted phosphoprotein 1 | 0 |
| *Spsb2* | splA/ryanodine receptor domain and SOCS box containing 2 | 0.023 |
| *Srgn* | serglycin | 0.041 |
| *Stat1* | signal transducer and activator of transcription 1 | 0 |
| *Stat2* | signal transducer and activator of transcription 2 | 0.002 |
| *Stat3* | signal transducer and activator of transcription 3 | 0.01 |
| *Stk10* | serine/threonine kinase 10 | 0.033 |
| *Stk39* | serine/threonine kinase 39, STE20/SPS1 homolog (yeast) | 0.086 |
| *Stxbp1* | syntaxin binding protein 1 | 0.046 |
| *Suclg2* | succinate-coenzyme A ligase, GDP-forming, beta subunit | 0.019 |
| *Sulf2* | sulfatase 2 | 0.009 |
| *Syt11* | synaptotagmin XI | 0.003 |
| *Sytl2_predicted* | synaptotagmin-like 2 (predicted) | 0.047 |
| *Tagln2* | transgelin 2 | 0.027 |
| *Tax1bp3* | Tax1 (human T-cell leukemia virus type I) binding protein 3 | 0.015 |
| *Tbrg1* | transforming growth factor beta regulated gene 1 | 0.044 |
| *Tcf19* | transcription factor 19 | 0.071 |
| *Tead3* | TEA domain family member 3 | 0.027 |

**TABLE 2 (CONTINUED). GENES FOUND TO HAVE SIGNIFICANTLY DIFFERENT TRANSCRIPT LEVELS AT SEVEN DAYS POSTDETACHMENT USING A FALSE DISCOVERY RATE (FDR) OF ≤0.1 (LISTED ALPHABETICALLY)**

| GENE SYMBOL | DESCRIPTION | FDR |
|---|---|---|
| *Tenc1_predicted* | tensin like C1 domain containing phosphatase (predicted) | 0.086 |
| *Tes* | testis derived transcript | 0.041 |
| *Tgfbi* | transforming growth factor, beta induced | 0.057 |
| *Tgfbr1* | transforming growth factor, beta receptor 1 | 0.05 |
| *Tgif1* | TG interacting factor 1 | 0.054 |
| *Tgm2* | transglutaminase 2, C polypeptide | 0.002 |
| *Thrsp* | thyroid hormone responsive protein | 0.087 |
| *Timp1* | tissue inhibitor of metalloproteinase 1 | 0 |
| *Timp2* | tissue inhibitor of metalloproteinase 2 | 0.02 |
| *Tm4sf1_predicted* | transmembrane 4 superfamily member 1 (predicted) | 0.045 |
| *Tmbim1* | transmembrane BAX inhibitor motif containing 1 | 0.003 |
| *Tmem123* | transmembrane protein 123 | 0.1 |
| *Tmem138* | transmembrane protein 138 | 0.086 |
| *Tmem16f_predicted* | transmembrane protein 16F (predicted) | 0.026 |
| *Tmem176a* | transmembrane protein 176A | 0 |
| *Tmem176b* | transmembrane protein 176B | 0.001 |
| *Tmem98* | transmembrane protein 98 | 0.097 |
| *Tmod1* | tropomodulin 1 | 0.014 |
| *Tnc* | Tenascin C | 0.05 |
| *Tnfaip6* | tumor necrosis factor alpha induced protein 6 | 0.004 |
| *Tnfrsf12a* | tumor necrosis factor receptor superfamily, member 12a | 0.086 |
| *Tnfrsf1a* | tumor necrosis factor receptor superfamily, member 1a | 0 |
| *Tpm1* | tropomyosin 1, alpha | 0.093 |
| *Tpm3* | tropomyosin 3, gamma | 0.003 |
| *Tpm4* | Tropomyosin 4 | 0.033 |
| *Tspan4* | tetraspanin 4 | 0.079 |
| *Tspo* | translocator protein | 0 |
| *Tst* | thiosulfate sulfurtransferase, mitochondrial | 0.07 |
| *Ttr* | transthyretin | 0.016 |
| *Tubb2b* | tubulin, beta 2b | 0.027 |
| *Twf1* | twinfilin, actin-binding protein, homolog 1 (Drosophila) | 0.087 |
| *Txnip* | thioredoxin interacting protein | 0.001 |
| *Tyrobp* | Tyro protein tyrosine kinase binding protein | 0.002 |
| *Ube2l6* | ubiquitin-conjugating enzyme E2L 6 | 0.009 |
| *Ube2n* | ubiquitin-conjugating enzyme E2N | 0.033 |
| *Usp18* | ubiquitin specific peptidase 18 | 0.088 |
| *Vamp8* | vesicle-associated membrane protein 8 | 0.068 |
| *Vasp_predicted* | vasodilator-stimulated phosphoprotein (predicted) | 0.08 |
| *Vax2* | ventral anterior homeobox containing gene 2 | 0.07 |
| *Vcam1* | vascular cell adhesion molecule 1 | 0.02 |
| *Vil2* | villin 2 | 0.044 |
| *Vim* | vimentin | 0.039 |
| *Wbp2* | WW domain binding protein 2 | 0.075 |
| *Wdr31* | WD repeat domain 31 | 0.028 |

**TABLE 2 (CONTINUED). GENES FOUND TO HAVE SIGNIFICANTLY DIFFERENT TRANSCRIPT LEVELS AT SEVEN DAYS POSTDETACHMENT USING A FALSE DISCOVERY RATE (FDR) OF ≤0.1 (LISTED ALPHABETICALLY)**

| GENE SYMBOL | DESCRIPTION | FDR |
|---|---|---|
| *Zfp238* | zinc finger protein 238 | 0.06 |
| *Zfp36l1* | zinc finger protein 36, C3H type-like 1 | 0.064 |
| *Zfp36l2* | zinc finger protein 36, C3H type-like 2 | 0.058 |

**TABLE 3. GENES FOUND TO HAVE SIGNIFICANTLY DIFFERENT TRANSCRIPT LEVELS AT 28 DAYS POSTDETACHMENT USING A FALSE DISCOVERY RATE (FDR) OF ≤0.1 (LISTED ALPHABETICALLY)**

| GENE SYMBOL | DESCRIPTION | FDR |
|---|---|---|
| *A2m* | alpha-2-macroglobulin | 0.068 |
| *Adfp* | adipose differentiation related protein | 0.083 |
| *Aif1* | allograft inflammatory factor 1 | 0.093 |
| *Ania4* | activity and neurotransmitter-induced early gene protein 4 (ania-4) | 0.014 |
| *Arpc1b* | actin related protein 2/3 complex, subunit 1B | 0.093 |
| *C1qa* | complement component 1, q subcomponent, alpha polypeptide | 0.023 |
| *C1qc* | complement component 1, q subcomponent, C chain | 0.031 |
| *C3* | complement component 3 | 0.023 |
| *Car3* | carbonic anhydrase 3 | 0.014 |
| *Ccnd1* | cyclin D1 | 0.038 |
| *Ccnd2* | cyclin D2 | 0.08 |
| *Cdr2* | cerebellar degeneration-related 2 | 0.093 |
| *Cebpd* | CCAAT/enhancer binding protein (C/EBP), delta | 0.088 |
| *Ctsc* | cathepsin C | 0.093 |
| *Ctss* | cathepsin S | 0.093 |
| *Ctsz* | cathepsin Z | 0.029 |
| *Edn2* | endothelin 2 | 0.093 |
| *Ednrb* | endothelin receptor type B | 0.033 |
| *Fam84a* | family with sequence similarity 84, member A | 0.065 |
| *Fcgr2b* | Fc receptor, IgG, low affinity IIb | 0.1 |
| *Fcgr3* | Fc receptor, IgG, low affinity III | 0.001 |
| *Fcgr3* | Fc receptor, IgG, low affinity III | 0.002 |
| *Fxyd3* | FXYD domain-containing ion transport regulator 3 | 0.065 |
| *Gal* | galanin | 0.001 |
| *Gbp2* | guanylate nucleotide binding protein 2 | 0.065 |
| *Gfap* | glial fibrillary acidic protein | 0.005 |
| *Gpnmb* | glycoprotein (transmembrane) nmb | 0.001 |
| *Hspb1* | heat shock protein 1 | 0.065 |
| *Ifitm2* | Interferon-induced transmembrane protein 2 | 0.08 |
| *Ifitm3* | Interferon-induced transmembrane protein 3 | 0.093 |
| *Laptm5* | lysosomal-associated protein transmembrane 5 | 0.033 |
| *Lcn2* | lipocalin 2 | 0.028 |
| *Lgals3* | lectin, galactose binding, soluble 3 | 0.02 |
| *Lgi2_predicted* | leucine-rich repeat LGI family, member 2 (predicted) | 0.002 |
| *Pdpn* | podoplanin | 0.028 |

**TABLE 3 (CONTINUED). GENES FOUND TO HAVE SIGNIFICANTLY DIFFERENT TRANSCRIPT LEVELS AT 28 DAYS POSTDETACHMENT USING A FALSE DISCOVERY RATE (FDR) OF ≤0.1 (LISTED ALPHABETICALLY)**

| GENE SYMBOL | DESCRIPTION | FDR |
|---|---|---|
| *S100a3* | S100 calcium-binding protein A3 | 0.002 |
| *S100a4* | S100 calcium-binding protein A4 | 0.037 |
| *Serpina3n* | serine (or cysteine) peptidase inhibitor, clade A, member 3N | 0.05 |
| *Serping1* | serine (or cysteine) peptidase inhibitor, clade G, member 1 | 0.014 |
| *Stat3* | signal transducer and activator of transcription 3 | 0.065 |
| *Tax1bp3* | Tax1 (human T-cell leukemia virus type I) binding protein 3 | 0.031 |
| *Timp1* | tissue inhibitor of metalloproteinase 1 | 0.067 |
| *Tmem176a* | transmembrane protein 176A | 0.01 |
| *Tmem176b* | transmembrane protein 176B | 0.079 |
| *Txnip* | thioredoxin interacting protein | 0.031 |

At the day 1 time point, 9 of the 44 genes (20%) found to have increased transcript levels are transcription factors. This is consistent with a previously published study of transcription factor levels after retinal detachment.[98] Other genes showing altered transcription levels at day 1 include genes coding for proteins involved in apoptosis, stress-response genes, and metabolism.

At 7 days after retinal-RPE separation, the number and categories of genes with increased transcription increase markedly from that seen at day 1. At this time point, gene categories showing increased transcription levels include inflammatory genes, immune-complex genes, antigen-presenting genes, stress-response genes, and metabolism genes. For example, there was increased transcription of various components of the complement 1 complex (genes *C1qa*, *C1qb*, *C1r*, and *C1s*). The genes for complement component 3 (*C3*), as well as for complement factor H (*Cfh*), also showed increased transcription. There is increased transcription of CD9, 44, 47, 48, 53, 63, 74, 99, 151, and 302, Stress-response genes showing detachment-induced increase in transcription include members of the annexin family *Anxa2*, *Anxa3*, *Anxa5*, and *Anxa7*, which code for annexin A2, A3, A5, and A7, respectively. These annexins are known regulators of cellular response to injury and apoptosis.[117] Crystallins are also highly activated after detachment, with crystalline alpha A (*Cryaa*), crystalline beta A1 (*Cryba1*), crystalline beta A2 (*Cryba2*), crystalline beta A4 (*Crya4*), crystalline beta B2 (*Crybb2*), and crystalline beta B3 (*Crybb3*) all showing increased transcription. Increased transcript levels for the genes coding for cathepsins C, H, S, and Z (*Ctsc*, *Ctsh*, *Ctss*, *Ctsz*), as well as lysozyme (*Lyz*) and the lysozomal membrane proteins Lamp2 and Laptm5, suggest a transcriptional activation of the autophagy pathway, a major stress-response/starvation-induced pathway that regulates cell survival. In the day 1 postdetachment arrays there was an activation of the gene coding for the interferon-dependent positive-acting transcription factor 3 gamma (*Isgf3g*). At the day 7 time point there are increased transcript levels for multiple interferon-dependent proteins (*Ifi27l*, *Ifi30*, *Ifitm1*, *Ifitm2*, *Ifitm3*, *Ifngr1*, *Ifngr2*, *Ifr1*, *Ifr7*), suggesting further activation of the interferon pathway in detached retinas. As in the day 1 array data, the day 7 arrays revealed that transcription factors themselves continued to show differential expression in detached vs attached retinas, suggesting continued regulation of gene transcription processes.

By the 28-day postdetachment time point, the number of differentially expressed genes drops off to just under 50. At this time point the gene categories showing differential expression are different from those seen at 1 and 7 days, with fewer transcription factors, metabolism, and acute stress-response genes having increased transcript levels, but rather more transcription of downstream executors and regulators of autophagy, inflammation, and intercellular signaling.

Notably, GFAP shows increased transcription in the detached vs attached retinas at all 3 time points tested. Müller cell hypertrophy and the corresponding increase in the levels of GFAP in these cells have been well demonstrated in the past.[32-34] The fact that our microarray results are consistent with this previously documented finding serves as a secondary internal control, suggesting that the transcription changes we detect reflect actual changes occurring within the detached retina.

When performing a 3×2 ANOVA on the set of arrays to account for the interaction effect of time of detachment (1 day, 7 days, or 28 days) vs attachment state (attached vs detached), 100 genes were identified as having significantly altered transcript levels with a FDR set at ≤0.1 (Table 4). When confining the analysis to the interaction effect to between days 1 and 7, a total of 144 genes were identified as significant with a FDR ≤0.1. Eighty-seven genes are common to both analyses. As with the individual day samples, the differentially expressed genes identified in the ANOVA analysis belonged to several main families of pathways, namely, transcription factors, stress-response genes, autophagy pathway–related genes, immune complex–related genes, and metabolism pathway genes.

**TABLE 4. RESULTS OF ANOVA ANALYSIS SHOWING GENES WITH SIGNIFICANTLY DIFFERENT TRANSCRIPT LEVELS AS A FUNCTION OF RETINAL STATE (ATTACHED VS DETACHED) AND TIME AFTER DETACHMENT (1, 7, AND 28 DAYS) USING A FALSE DISCOVERY RATE (FDR) OF ≤0.1 (LISTED ALPHABETICALLY)***

| GENE SYMBOL | GENE NAME | DAYS 1, 7, AND 28 ANOVA FDR | DAYS 1 AND 7 ANOVA FDR |
|---|---|---|---|
| *A2m* | alpha-2-macroglobulin | 0.0139 | 0.008 |
| *Acadl* | acetyl-coenzyme A dehydrogenase, long-chain | | 0.0687 |
| *Adipor2* | adiponectin receptor 2 | 0.0455 | |
| *Aif1* | allograft inflammatory factor 1 | 0.0006 | 0 |
| *Akap13* | a kinase (prka) anchor protein 13 | | 0.0401 |
| *Anxa3* | annexin A3 | | 0.0024 |
| *Apbb1ip (predicted)* | amyloid beta (A4) precursor protein-binding, family B, member 1 interacting protein (predicted) | | 0.0153 |
| *Arhgdib (predicted)* | rho, GDP dissociation inhibitor (GDI) beta (predicted) | | 0.0705 |
| *Arpc1b* | actin-related protein 2/3 complex, subunit 1B | 0.0912 | |
| *Asns* | asparagine synthetase | 0.023 | |
| *Ass* | arginosuccinate synthetase | | 0.0667 |
| *Atf3* | activating transcription factor 3 | 0.0052 | |
| *Atf5* | activating transcription factor 5 | 0.0031 | 0.0028 |
| *B2m* | beta-2 microglobulin | | 0.0954 |
| *B4galt5 (predicted)* | udp-gal:betaglcnac beta 1,4-galactosyltransferase, polypeptide 5 (predicted) | 0.0937 | 0.0142 |
| *Bclaf1* | BCL2-associated transcription factor 1 (predicted) | 0.0697 | 0.0759 |
| *Best5* | bone-expressed sequence tag 5 protein | | 0.0226 |
| *Bzrp* | benzodiazepin receptor | | 0.0787 |
| *C1qa* | complement component 1, q subcomponent, alpha polypeptide | 0.001 | 0.0001 |
| *C1qb* | complement component 1, q subcomponent, beta polypeptide | | 0.0004 |
| *C1qg (predicted)* | complement component 1, q subcomponent, gamma polypeptide (predicted) | 0.01 | 0.0031 |
| *C1r (predicted)* | complement component 1, r subcomponent (predicted) | | 0.0474 |
| *C3* | complement component 3 | 0.0018 | 0 |
| *C4a* | complement component 4a | 0.0107 | 0.0009 |
| *Ca3* | carbonic anhydrase 3 | 0.0049 | 0 |
| *Carhsp1* | calcium regulated heat stable protein 1 | | 0.0954 |
| *Cars (predicted)* | cysteinyl-tRNA synthetase (predicted) | 0.011 | |
| *Cd53* | CD53 antigen | 0.0202 | 0.0002 |
| *Cd68* | CD68 antigen | | 0.0846 |
| *Cd74* | CD74 antigen (invariant polpypeptide of major histocompatibility class II antigen-associated) | 0.0143 | 0.0002 |

**TABLE 4 (CONTINUED). RESULTS OF ANOVA ANALYSIS SHOWING GENES WITH SIGNIFICANTLY DIFFERENT TRANSCRIPT LEVELS AS A FUNCTION OF RETINAL STATE (ATTACHED VS DETACHED) AND TIME AFTER DETACHMENT (1, 7, AND 28 DAYS) USING A FALSE DISCOVERY RATE (FDR) OF ≤0.1 (LISTED ALPHABETICALLY)***

| GENE SYMBOL | GENE NAME | DAYS 1, 7, AND 28 ANOVA FDR | DAYS 1 AND 7 ANOVA FDR |
|---|---|---|---|
| *Cd9* | CD9 antigen | | 0.0589 |
| *Cdh13* | cadherin 13 | | 0.0056 |
| *Cish* | cytokine inducible SH2-containing protein | | 0.0134 |
| *Clrb (predicted)* | Similar to osteoclast inhibitory lectin | | 0.0448 |
| *Cnp1* | cyclic nucleotide phosphodiesterase 1 | | 0.0621 |
| *Cntf* | ciliary neurotrophic factor | | 0.0585 |
| *Coro1a* | coronin, actin-binding protein 1A | 0.0169 | 0.0341 |
| *Cp* | ceruloplasmin | | 0.0435 |
| *Csf1r* | colony stimulating factor 1 receptor | 0.0002 | 0 |
| *Csrp1* | cysteine and glycine-rich protein 1 | 0.0597 | 0.0371 |
| *Ctsh* | cathepsin H | 0.011 | 0.0356 |
| *Ctss* | cathepsin S | 0.0068 | 0.0153 |
| *Ctsz* | cathepsin Z | 0.0578 | 0.0009 |
| *Dap* | death-associated protein | | 0.0629 |
| *Dtx3l_similar* | similar to deltex 3-like | 0 | 0 |
| *Edg3* | transcribed locus | | 0.0468 |
| *Egfr* | epidermal growth factor receptor | | 0.0003 |
| *Elk3 (predicted)* | ELK3, member of ETS oncogene family (predicted) | 0.0145 | 0.0005 |
| *Eps15 (predicted)* | epidermal growth factor receptor pathway substrate 15 (predicted) | | 0.0448 |
| *Fcgr3* | Fc receptor III | 0.0243 | 0.0267 |
| *Fcgr3a* | Fc fragment of IgG, low affinity IIIa, receptor for (CD16) | 0.0076 | 0 |
| *Fgf2* | fibroblast growth factor 2 | 0.0019 | 0.0072 |
| *Ftl1* | ferritin light chain 1 | | 0.0954 |
| *Fxyd3* | FXYD domain-containing ion transport regulator 3 | 0.0021 | 0.0011 |
| *Fxyd5* | FXYD domain-containing ion transport regulator 5 | | 0.0042 |
| *Gal* | galanin | 0 | 0 |
| *Gldc (predicted)* | glycine dehydrogenase (decarboxylating; glycine decarboxylase, glycine cleavage system protein P) (predicted) | 0.0964 | 0.0185 |
| *Gnb3* | guanine nucleotide binding protein, beta 3 | | 0.0525 |
| *Gpm6b* | glycoprotein m6b | 0.0177 | 0.0117 |
| *Gpnmb* | glycoprotein (transmembrane) nmb | 0.0002 | 0 |
| *Gpr56* | G protein-coupled receptor 56 | | 0.0267 |
| *Grn* | granulin | 0.0022 | 0.0015 |

**TABLE 4 (CONTINUED). RESULTS OF ANOVA ANALYSIS SHOWING GENES WITH SIGNIFICANTLY DIFFERENT TRANSCRIPT LEVELS AS A FUNCTION OF RETINAL STATE (ATTACHED VS DETACHED) AND TIME AFTER DETACHMENT (1, 7, AND 28 DAYS) USING A FALSE DISCOVERY RATE (FDR) OF ≤0.1 (LISTED ALPHABETICALLY)***

| GENE SYMBOL | GENE NAME | DAYS 1, 7, AND 28 ANOVA FDR | DAYS 1 AND 7 ANOVA FDR |
|---|---|---|---|
| *Gstt3 (predicted)* | similar to glutathione S-transferase, theta 3 (predicted) | 0.0008 | 0.0018 |
| *Hadhsc* | L-3-hydroxyacyl-coenzyme A dehydrogenase, short chain | 0.048 | 0.0442 |
| *Hla-dma* | major histocompatibility complex, class II, DM alpha | 0.0166 | 0.0015 |
| *Hla-dmb* | major histocompatibility complex, class II, DM beta | 0.048 | 0.0091 |
| *hypothetical LOC289313* | hypothetical LOC289313 | 0.0019 | 0.023 |
| *Icam1* | intercellular adhesion molecule 1 | 0 | 0 |
| *Ifi30 (predicted)* | interferon gamma inducible protein 30 (predicted) | 0.0081 | 0.0083 |
| *Ifitm1 (predicted)* | interferon induced transmembrane protein 1 (predicted) | 0.048 | 0.0448 |
| *Ifitm2* | interferon induced transmembrane protein 2 (1-8D) | 0.0873 | 0.009 |
| *Ifngr* | interferon gamma receptor 1 | 0.0274 | 0.0103 |
| *Igf1* | insulin-like growth factor 1 | | 0.0623 |
| *Igtp* | interferon gamma induced GTPase | 0.0435 | 0.0153 |
| *Iqgap1 (predicted)* | IQ motif containing GTPase activating protein 1 (predicted) | | 0.0351 |
| *Irf1* | interferon regulatory factor 1 | 0.0455 | 0.0448 |
| *Kctd12 (predicted)* | potassium channel tetramerisation domain containing 12 (predicted) | 0.0655 | 0.0525 |
| *Laptm5* | lysosomal-associated protein transmembrane 5 | 0.0002 | 0.0003 |
| *Lcn2* | lipocalin 2 | 0.0024 | 0 |
| *Lcp1 (predicted)* | lymphocyte cytosolic protein 1 (predicted) | | 0.0437 |
| *Leprel2 (predicted)* | leprecan-like 2 (predicted) | 0.0179 | |
| *Lgals3* | lectin, galactose binding, soluble 3 | | 0.0401 |
| *Lgals3bp* | lectin, galactoside-binding, soluble, 3 binding protein | 0.0018 | 0 |
| *Lgi2 (predicted)* | leucine-rich repeat LGI family, member 2 (predicted) | 0 | 0.0077 |
| *LOC313410* | similar to methylenetetrahydrofolate dehydrogenase (NAD) (EC 1.5.1.15) / methenyltetrahydrofolate cyclohydrolase (EC 3.5.4.9) precursor-mouse | | 0.0001 |
| *LOC498279* | similar to NADH dehydrogenase (ubiquinone) Fe-S protein 2 | 0.0044 | 0.0047 |
| *Lyz* | lysozyme | 0.0456 | 0.0027 |

**TABLE 4 (CONTINUED). RESULTS OF ANOVA ANALYSIS SHOWING GENES WITH SIGNIFICANTLY DIFFERENT TRANSCRIPT LEVELS AS A FUNCTION OF RETINAL STATE (ATTACHED VS DETACHED) AND TIME AFTER DETACHMENT (1, 7, AND 28 DAYS) USING A FALSE DISCOVERY RATE (FDR) OF ≤0.1 (LISTED ALPHABETICALLY)***

| GENE SYMBOL | GENE NAME | DAYS 1, 7, AND 28 ANOVA FDR | DAYS 1 AND 7 ANOVA FDR |
|---|---|---|---|
| *Maf* | V-maf musculoaponeurotic fibrosarcoma (avian) oncogene homolog (c-maf) | 0.048 | 0.0585 |
| *Mak10* | MAK10 homolog, amino-acid N-acetyltransferase subunit, (S. cerevisiae) | 0.0024 | 0.0003 |
| *Mars (predicted)* | methionine-tRNA synthetase (predicted) | 0.044 | |
| *Matn2 (predicted)* | matrilin 2 (predicted) | 0.0647 | 0.0131 |
| *Mmp14* | matrix metalloproteinase 14 (membrane-inserted) | 0.0578 | 0.006 |
| *Mpeg1* | macrophage expressed gene 1 | 0.0362 | 0.0009 |
| *Notch1* | Notch gene homolog 1 (Drosophila) | 0.0202 | 0.0036 |
| *Notch2* | Notch gene homolog 2 (Drosophila) | | 0.0226 |
| *Npc2* | Niemann Pick type C2 | 0.0274 | 0.0614 |
| *Olfml3 (predicted)* | olfactomedin-like 3 (predicted) | | 0.0506 |
| *Opn4* | opsin 4 (melanopsin) | 0.0414 | 0.0267 |
| *P2ry12* | transcribed locus | 0.0975 | 0.0274 |
| *Paqr8* | progestin and adipoQ receptor family member VIII | 0.0455 | 0.0484 |
| *Pcsk2* | proprotein convertase subtilisin/kexin type 2 | | 0.0956 |
| *Pla2g4a* | phospholipase A2, group IVA (cytosolic, calcium-dependent) | | 0.047 |
| *Plac8 (predicted)* | placenta-specific 8 (predicted) | 0.0367 | 0 |
| *Pld4* | phospholipase D family, member 4 | | 0.0039 |
| *Postn (predicted)* | periostin, osteoblast specific factor (predicted) | 0.0147 | 0.0014 |
| *Prickle2 (predicted)* | prickle-like 2 (Drosophila) (predicted) | | 0.0575 |
| *Psmb8* | proteosome (prosome, macropain) subunit, beta type 8 | 0.0052 | 0 |
| *Psmb9* | proteosome (prosome, macropain) subunit, beta type 9 | 0.001 | 0.011 |
| *Ptn* | pleiotrophin | 0.026 | 0.0751 |
| *Ptpns1* | protein tyrosine phosphatase, nonreceptor type substrate 1 | | 0.0882 |
| *Ptprc* | protein tyrosine phosphatase, receptor type, C | 0.026 | 0.0621 |
| *Rab3b* | RAB3B, member RAS oncogene family | | 0.0612 |
| *Raly* | hnRNP-associated with lethal yellow | | 0.047 |
| *RGD1306410* | similar to CG14980-PB | 0.0991 | |
| *RGD1306534 (predicted)* | similar to P-Rex1 (predicted) | 0.0199 | 0.0083 |

**TABLE 4 (CONTINUED). RESULTS OF ANOVA ANALYSIS SHOWING GENES WITH SIGNIFICANTLY DIFFERENT TRANSCRIPT LEVELS AS A FUNCTION OF RETINAL STATE (ATTACHED VS DETACHED) AND TIME AFTER DETACHMENT (1, 7, AND 28 DAYS) USING A FALSE DISCOVERY RATE (FDR) OF ≤0.1 (LISTED ALPHABETICALLY)***

| GENE SYMBOL | GENE NAME | DAYS 1, 7, AND 28 ANOVA FDR | DAYS 1 AND 7 ANOVA FDR |
|---|---|---|---|
| *RGD1310323* | similar to RIKEN cDNA 1200004M23 | | 0.0954 |
| *RGD1559694 (predicted)* | transcribed locus | | 0.0086 |
| *RGD1560925 (predicted)* | similar to 2610034M16Rik protein (predicted) | 0.0846 | 0.0251 |
| *RGD1564045 (predicted)* | RGD1564045 (predicted) | | 0.0681 |
| *RGD1566254 (predicted)* | LOC499318 | 0.0002 | 0 |
| *Rgs10* | regulator of G-protein signalling 10 | | 0.0954 |
| *Ril* | reversion induced LIM gene | 0.0138 | 0.0002 |
| *RT1-Bb* | RT1 class II, locus Bb | 0.0144 | 0.0153 |
| *RT1-CE5* | RT1 class I, CE5 | 0.0098 | 0.0051 |
| *RT1-Da* | RT1 class II, locus Da | 0.0107 | 0 |
| *RT1-S3* | RT1 class Ib, locus S3 | 0.0021 | 0.0019 |
| *S100a3* | S100 calcium-binding protein A3 | 0.0003 | 0.0006 |
| *S100a4* | S100 calcium-binding protein A4 | | 0.0685 |
| *S100b* | S100 protein, beta polypeptide | 0.0597 | 0.0621 |
| *Sema5a (predicted)* | sema domain, seven thrombospondin repeats (type 1 and type 1-like), transmembrane domain (TM) and short cytoplasmic domain, (semaphorin) 5A (predicted) | 0.0435 | 0.039 |
| *Serpina3n* | serine (or cysteine) peptidase inhibitor, clade A, member 3N | | 0.0142 |
| *Serpinb1a* | serine (or cysteine) proteinase inhibitor, clade B, member 1a | 0.0259 | |
| *Serping1* | serine (or cysteine) peptidase inhibitor, clade G, member 1 | 0.0011 | 0.0004 |
| *Slc1a3* | solute carrier family 1 (glial high affinity glutamate transporter), member 3 | 0.0455 | 0.0401 |
| *Slc44a2 (predicted)* | solute carrier family 44, member 2 (predicted) | | 0.0153 |
| *SP110* | SP110 nuclear body protein | | 0.0004 |
| *Sparc* | secreted acidic cysteine rich glycoprotein | | 0.0759 |
| *Spp1* | secreted phosphoprotein 1 | 0.0579 | 0.0057 |
| *Stat2 (predicted)* | signal transducer and activator of transcription 2 (predicted) | 0.0065 | 0.0705 |
| *Stk10* | serine/threonine kinase 10 | | 0.0525 |
| *Suclg2 (predicted)* | succinate-coenzyme A ligase, GDP-forming, beta subunit (predicted) | | 0.0882 |
| *Tap1* | transporter 1, ATP-binding cassette, sub-family B (MDR/TAP) | 0.0001 | 0.0331 |
| *Tars* | threonyl-tRNA synthetase | 0.0293 | |
| *Tgm2* | transglutaminase 2, C polypeptide | 0.0107 | 0.0442 |

**TABLE 4 (CONTINUED). RESULTS OF ANOVA ANALYSIS SHOWING GENES WITH SIGNIFICANTLY DIFFERENT TRANSCRIPT LEVELS AS A FUNCTION OF RETINAL STATE (ATTACHED VS DETACHED) AND TIME AFTER DETACHMENT (1, 7, AND 28 DAYS) USING A FALSE DISCOVERY RATE (FDR) OF ≤0.1 (LISTED ALPHABETICALLY)***

| GENE SYMBOL | GENE NAME | DAYS 1, 7, AND 28 ANOVA FDR | DAYS 1 AND 7 ANOVA FDR |
|---|---|---|---|
| *Timp1* | tissue inhibitor of metalloproteinase 1 | | 0.0092 |
| *Tmem176a* | transmembrane protein 176A | 0.0097 | 0.0095 |
| *Tmem176b* | transmembrane protein 176B | 0.0687 | 0.0685 |
| *Tmod1* | tropomodulin 1 | | 0.0437 |
| *Tnfaip6* | tumor necrosis factor alpha induced protein 6 | | 0.0648 |
| *Trib3* | tribbles homolog 3 (Drosophila) | | 0.047 |
| *Txnip* | thioredoxin interacting protein | 0.0014 | 0.001 |
| *Tyrobp* | Tyro protein tyrosine kinase binding protein | 0.001 | 0.0001 |
| *Vasp (predicted)* | vasodilator-stimulated phosphoprotein (predicted) | 0.0655 | |
| *Vcam1* | vascular cell adhesion molecule 1 | 0.0524 | 0.017 |
| *Yars* | tyrosyl-tRNA synthetase | 0.0245 | |
| *Zfp423* | zinc finger protein 423 | 0.0167 | |
| *Zfp655* | zinc finger protein 655 | 0.0597 | 0.0401 |

*A total of 100 genes were found to have significantly altered transcript levels using all 3 time points, and 144 genes when using only the days 1 and 7 time points. Eighty-seven genes were common to both analyses

Another way of looking at the ANOVA results is shown in Figures 2 and 3. These figures present the data in a graphic, color-coded manner known as a "heatmap." In these heatmaps, the arrays, listed on the top, are ordered as a function of time after detachment. Also, the control arrays corresponding to attached retinas are placed to the left, and the arrays corresponding to the detached retinas are placed to the right. The more similar the transcript level, the more similar the color will be across the different arrays. Changes in color represent a change in the transcript level. For example, looking at the color pattern for the gene denoted CD53, the colors are mostly blue in all the attached, control retinas, corresponding to low transcription levels. The transcript level remains relatively low at 1 day postdetachment, but the color turns markedly darker at day 7 postdetachment and stays dark through the day 28 time point. This corresponds to an increasing transcript level that remains elevated through the final time point. The genes are arranged according to a "clustering" algorithm that puts genes with the most similar temporal transcription changes closest together, and those with the most dissimilar profiles farthest from each other. Figure 2 shows the heatmap for the complete data set, and Figure 3 gives the heatmap for the days 1 and 7 time points only.

To confirm the transcript changes detected on the microarray chips, we performed qRT-PCR using high-efficiency microfluidics cards. In qRT-PCR assays, the actual level of the mRNA transcript is measured, providing independent confirmation of differential transcript levels observed with the microarrays. The retinas tested for the qRT-PCR validation were different from the ones used for the microarray assays, providing an extra level of independence to the validation. For the microfluidic qRT-PCR we used the Applied Biosystem Corporation TaqMan low density array (TLDA) assay. This assay uses a rapid, microfluidic system that allows for testing many independent genes at the same time. We confirmed the transcript level for 51 genes that were found to be significantly altered in their transcript profiles between days 1 and 7 on the ANOVA analysis (Table 5). The mRNA for the TLDA assay was taken from retinas detached for 7 days. Table 5 shows the results for this analysis. For all 51 genes tested, the TLDA assay confirmed that the transcript level detected on the microarray was correct in both direction (increased transcription) and relative magnitude (amount of increase). We recognize, however, that the validation of the microarray results with qRT-PCR may not reflect changes in actual protein levels.

The gene with the largest increase in transcription, as found by the ANOVA analysis and confirmed with the TLDA, was the one encoding for the protein lipocalin 2 (*Lcn2*). This gene showed a 141-fold increase in transcription at 7 days after retinal detachment. The gene with the next highest increase in transcript level was the one encoding for galectin-3 (*Lgals3*), a member of a family of beta-galactoside-binding animal lectins, which had a 96-fold increase in its transcript level. Rounding out the list of the top 5 genes with the largest increases in transcript levels were the tissue inhibitor of metalloproteinase 1 (*Timp1*) with a 57-fold increase in its transcript level, carbonic anhydrase 3 (*Ca3*) with a 46-fold increase, serine peptidase inhibitor (*Serpina3n*) with a 45-fold increase, and galanin (*gal*) with a 31-fold increase.

## MAP KINASE ACTIVATION

A prototypical transducer of stress-stimuli is the family of kinases known as the mitogen-activated protein kinases, or MAP kinases.[118-120] The family of MAP kinases has 3 main branches, each of which can become active during periods of cell stress: the p38 kinase, the Jun N-terminal kinase (JNK), and the p42/p44 kinase. Activation of the MAP kinases results in modification of gene transcription. As such, we hypothesized that there would be an early activation of at least one of the branches of the MAP kinase family in response to retinal-RPE separation, a significant stress signal to the retina.

Figures 4 and 5 show the results for the Western blot analysis of p38 kinase and the JNK activation, respectively. As can be seen, there is no detachment-induced change in the levels of phosphorylated (ie, activated) protein for either of these 2 kinases. In contrast, there is a significant increase in the amount of phosphorylated p42/p44 kinase early after retinal-RPE separation (Figure 6). There is no major change in the level of total protein, suggesting that it is the preexisting pool of p42/p44 kinase that is being phosphorylated.

Activation of the p42/p44 MAP kinase occurs through the upstream activity of a specific MAP kinase kinase known as MEK. We tested the ability of 2 known inhibitors of MEK, PD98059 and U0126, to prevent the detachment-induced phosphorylation of the MAP kinase. The 2 inhibitors were delivered either into the subretinal space itself or into the peritoneal cavity at the time the detachment was created. As can be seen in Figure 7, both PD98059 and U0126 were able to prevent the detachment-induced increase in phosphorylated p42/p44 kinase. Again, there was no change in the level of total p42/p44 (data not shown). Injection of the delivery solvent (DMSO) alone did not prevent the detachment-induced increase in phosphorylated p42/p44 kinase.

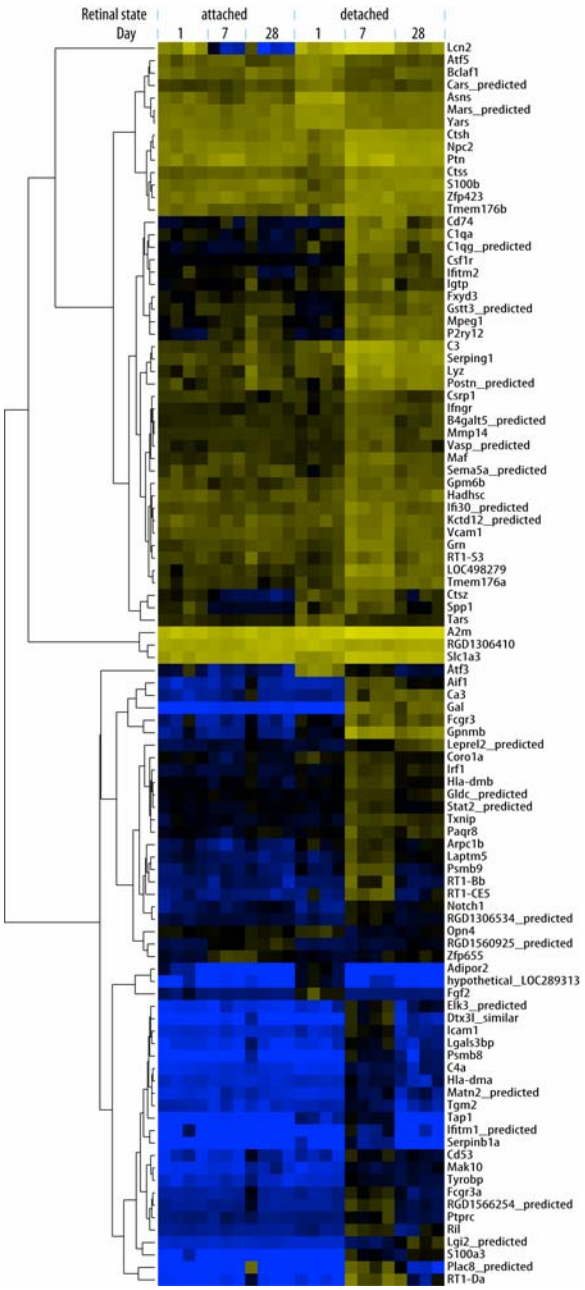


**FIGURE 2**

Heatmap of the ANOVA results showing genes with significantly altered transcription levels as a function of attachment state and time of detachment. For this analysis all 3 time points (1 day, 7 days, and 28 days postdetachment) were included. Genes are arranged according to a clustering algorithm that places the genes with the most similar pattern of transcription level closest to each other.

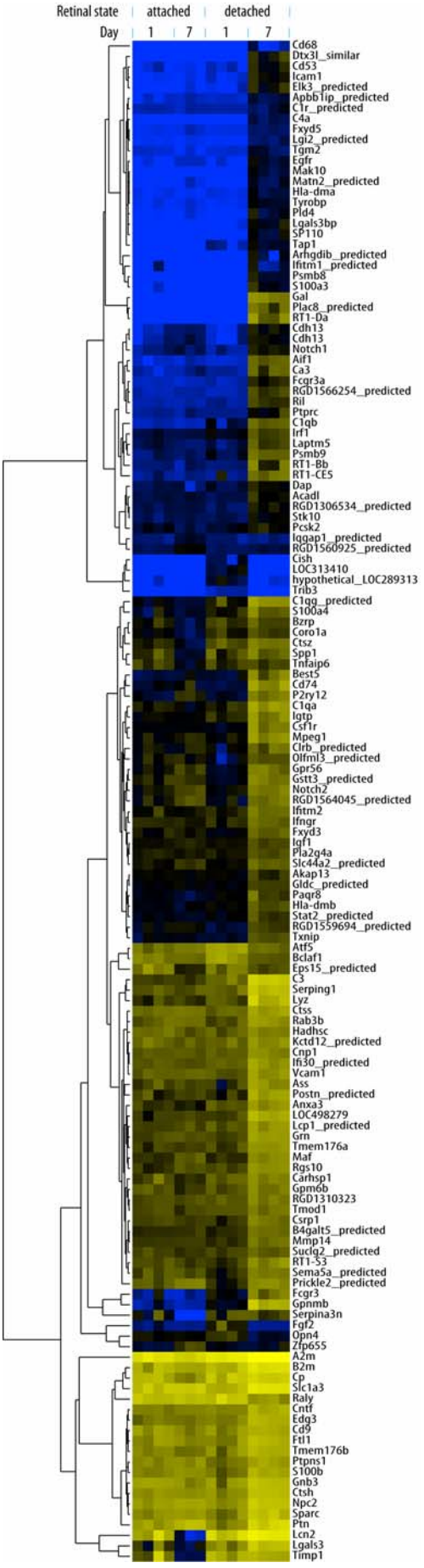


**FIGURE 3**

Heatmap of the ANOVA results showing genes with significantly altered transcription levels as a function of attachment state and time of detachment. For this analysis only the 1-day and 7-day postdetachment time points were included. Genes are arranged according to a clustering algorithm that places the genes with the most similar pattern of transcription level closest to each other.

**TABLE 5. CHANGE OBSERVED IN 51 GENES AT DAY 7 POSTDETACHMENT: ANALYSIS BY TLDA ASSAY AND MICROARRAY (LISTED IN DESCENDING ORDER OF "-FOLD" CHANGE DETECTED ON TLDA)***

| GENE SYMBOL | GENE NAME | TLDA MEAN "-FOLD" CHANGE | DAY 7 MICROARRAY "-FOLD" CHANGE |
|---|---|---|---|
| *Lcn2* | lipocalin 2 | 141.20 | 711.04 |
| *Lgals3* | lectin, galactose binding, soluble 3 | 96.10 | 72.45 |
| *Timp1* | tissue inhibitor of metalloproteinase 1 | 56.92 | 81.79 |
| *Ca3* | carbonic anhydrase 3 | 45.57 | 23.44 |
| *Serpina3n* | serine (or cysteine) peptidase inhibitor, clade A, member 3N | 44.91 | 55.46 |
| *Gpnmb* | glycoprotein (transmembrane) nmb | 31.19 | 288.45 |
| *Gal* | galanin | 30.27 | 185.39 |
| *C3* | complement component 3 | 21.86 | 26.98 |
| *Lyz* | lysozyme | 20.71 | 20.12 |
| *Fcgr3a* | Fc fragment of IgG, low affinity IIIa, receptor for (CD16) | 19.35 | 13.86 |
| *Cd74* | CD74 antigen (invariant polpypeptide of major histocompatibility class II antigen-associated) | 18.73 | 14.39 |
| *Serping1* | serine (or cysteine) peptidase inhibitor, clade G, member 1 | 16.32 | 11.84 |
| *C1qg (predicted)* | complement component 1, q subcomponent, gamma polypeptide (predicted) | 15.95 | 35.48 |
| *Psmb9* | proteosome (prosome, macropain) subunit, beta type 9 | 15.54 | 21.15 |
| *S100a4* | S100 calcium-binding protein A4 | 14.54 | 13.28 |
| *C1qb* | complement component 1, q subcomponent, beta polypeptide | 14.11 | 46.19 |
| *Tyrobp* | Tyro protein tyrosine kinase binding protein | 13.95 | 7.09 |
| *Fcgr3* | Fc receptor, IgG, low affinity III | 13.55 | 35.29 |
| *Psmb8* | proteosome (prosome, macropain) subunit, beta type 8 | 13.21 | 19.29 |
| *Tap1* | transporter 1, ATP-binding cassette, sub-family B (MDR/TAP) | 12.52 | 12.64 |
| *Cp* | ceruloplasmin | 11.97 | 5.88 |
| *Cd53* | CD53 antigen | 11.14 | 17.3 |
| *A2m* | alpha-2-macroglobulin | 10.44 | 4.62 |
| *Bzrp* | benzodiazepin receptor | 9.85 | 8.83 |
| *Aif1* | allograft inflammatory factor 1 | 9.57 | 42.62 |
| *C4a* | complement component 4a | 9.32 | 4.57 |
| *S100a3* | S100 calcium-binding protein A3 | 8.75 | 35.81 |
| *C1qa* | complement component 1, q subcomponent, alpha polypeptide | 8.70 | 23.4 |
| *Lgals3bp* | lectin, galactoside-binding, soluble, 3 binding protein | 8.59 | 15.72 |
| *Laptm5* | lysosomal-associated protein transmembrane 5 | 8.55 | 13.89 |
| *Ril* | reversion induced LIM gene | 8.47 | 16.85 |
| *Fxyd5* | FXYD domain-containing ion transport regulator 5 | 8.40 | 2.52 |
| *B2m* | beta-2 microglobulin | 7.84 | 5.15 |
| *Icam1* | intercellular adhesion molecule 1 | 7.78 | 16.86 |
| *Irf1* | interferon regulatory factor 1 | 7.32 | 8.11 |

**TABLE 5 (CONTINUED). CHANGE OBSERVED IN 51 GENES AT DAY 7 POSTDETACHMENT: ANALYSIS BY TLDA ASSAY AND MICROARRAY (LISTED IN DESCENDING ORDER OF "-FOLD" CHANGE DETECTED ON TLDA)***

| GENE SYMBOL | GENE NAME | TLDA MEAN "-FOLD" CHANGE | DAY 7 MICROARRAY "-FOLD" CHANGE |
|---|---|---|---|
| *Anxa3* | annexin A3 | 7.20 | 11.31 |
| *Arpc1b* | actin-related protein 2/3 complex, subunit 1B | 6.95 | 17.31 |
| *Ctsz* | cathepsin Z | 6.64 | 16.78 |
| *Carhsp1* | calcium regulated heat stable protein 1 | 6.61 | 5.82 |
| *Tmem176b* | transmembrane protein 176B | 5.74 | 4.5 |
| *Ifitm2* | interferon-induced transmembrane protein 2 (1-8D) | 5.49 | 6.06 |
| *Hla-dma* | major histocompatibility complex, class II, DM alpha | 4.78 | 6.59 |
| *Aft3* | activating transcription factor 3 | 4.67 | 7.42 |
| *Grn* | granulin | 4.13 | 4.94 |
| *Ctsh* | cathepsin H | 4.11 | 3.15 |
| *Ctss* | cathepsin S | 3.71 | 2.67 |
| *Ifngr* | interferon gamma receptor 1 | 2.94 | 4.06 |
| *Fxyd3* | FXYD domain-containing ion transport regulator 3 | 2.77 | 3.99 |
| *Cdh13* | cadherin 13 | 2.47 | 4.52 |
| *Asns* | asparagine synthetase | 1.98 | 2.74 |
| *Gpr56* | G protein-coupled receptor 56 | 1.79 | 2.96 |

TLDA, TaqMan low-density array.

*Fifty-one genes found to have differentially expressed transcript levels between days 1 and 7 postdetachment had the transcript levels validated using TLDA microfluidic quantitative real-time polymerase chain reaction assay.

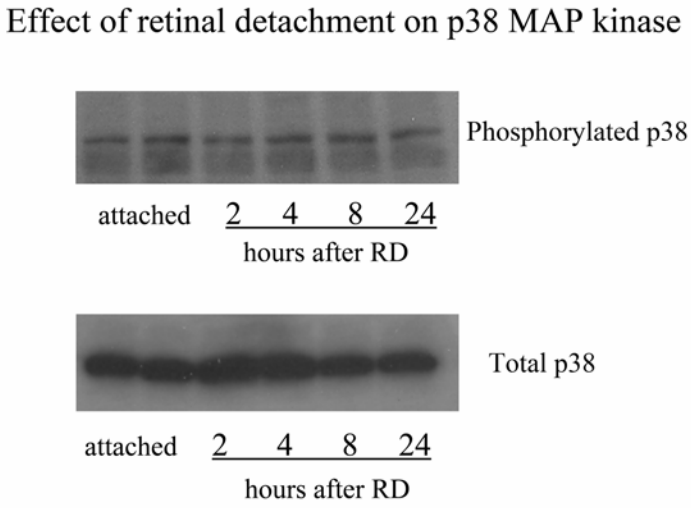


**FIGURE 4**

Effect of retinal detachment on levels of p38 mitogen-activated protein (MAP) kinase. Immunoblot analysis of the total vs phosphorylated levels of p38 kinase in attached vs detached retinas. Retinas were harvested at 2, 4, 8, and 24 hours after retinal detachment (RD). There was no change in either the total p38 level or in the level of phosphorylated p38 at any of the time points sampled. Equal loading across lanes was confirmed with Ponceau S staining and densitometry analysis of a nonspecific IgG band (not shown).

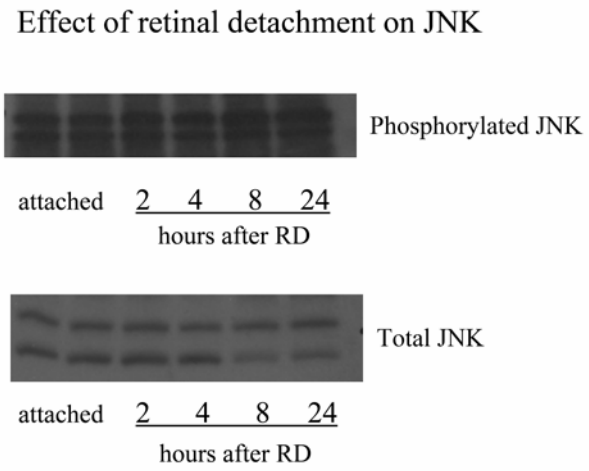


**FIGURE 5**

Effect of retinal detachment on levels of Jun N-terminal kinase (JNK). Immunoblot analysis of the total vs phosphorylated levels of JNK in attached vs detached retinas. Retinas were harvested at 2, 4, 8, and 24 hours after retinal detachment (RD). There was no change in either the total JNK or in the level of phosphorylated JNK at any of the time points sampled. Equal loading across lanes was confirmed with Ponceau S staining and densitometry analysis of a nonspecific IgG band (not shown).

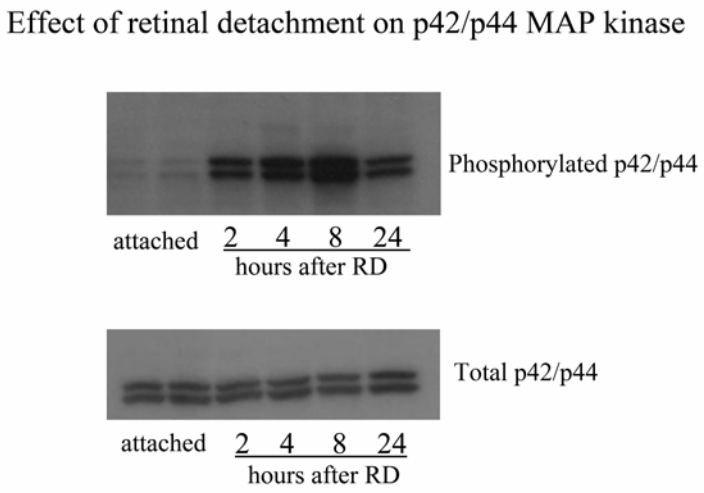


**FIGURE 6**

Effect of retinal detachment on levels of p42/p44 mitogen activated protein (MAP) kinase. Immunoblot analysis of the total vs phosphorylated levels of p42/p44 kinase in attached vs detached retinas. Retinas were harvested at 2, 4, 8, and 24 hours after retinal detachment (RD). There was a marked increase in the level of phosphorylated p42/p44 after retinal detachment even as early as 2 hours postdetachment. There was no change in the total p42/p44 levels, suggesting that the phosphorylated kinase derived from the total pool of kinases, rather than de novo synthesis of new protein. Equal loading across lanes was confirmed with Ponceau S staining and densitometry analysis of a nonspecific IgG band (not shown).

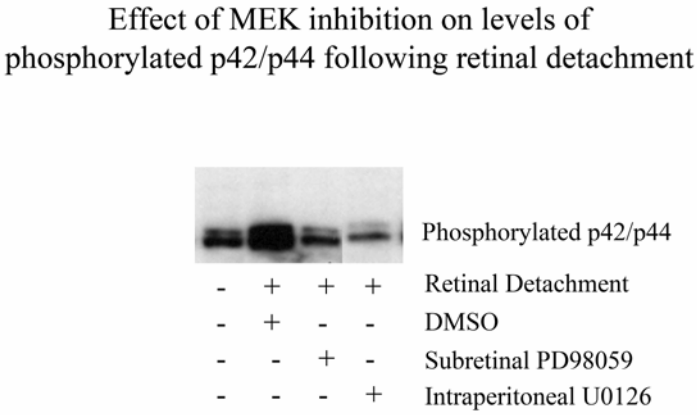


**FIGURE 7**

Inhibition of mitogen-activated protein (MAP) kinase phosphorylation by the subretinal or intraperitoneal administration of the compounds PD98059 and U0126 results in decreased levels of phosphorylated p42/p44 after retinal detachment. Both PD98059 and U0126 are specific inhibitors of MEK, the protein responsible for p42/p44 phosphorylation. DMSO, dimethyl sulfoxide.

## DISCUSSION

The data presented in this thesis show that separation of the neurosensory retina from the underlying RPE results in a significant change in the gene transcription profile of the retina. As we predicted from our original hypothesis, the number and type of genes transcribed within the retina vary not only as a function of detachment, but also as a function of time of detachment. Many of the genes showing differential transcription in the detached retina belong to pathways known to regulate the types of morphologic and functional changes known to occur in detached retinas. In addition, many unique genes were shown to have differential expression. Finally, we were able to show that there was activation of the p42/p44 stress-response MAP kinase very early after retinal-RPE separation.

Analysis of the retinal gene transcription profile shows an early increase in transcription factor expression at day 1 postdetachment. Given that transcription factors control the transcription of other genes, it is not surprising that there is a 10-fold increase in the number of genes being differentially expressed at day 7 postdetachment. An example of a transcription factor with early activation leading to an increase in the transcript level of one of its known downstream targets would be activating transcription factor 3 (*Atf3*). At day 1 postdetachment, the microarray showed a significant increase in the level of *Atf3* transcript. At day 7 postdetachment, there is an increase in cyclin D1 (*Ccnd1*), a regulator of mitosis and a gene whose transcription is regulated by *Atf3*.[121] Another example would be the gene *Hspb1* that codes for a gene called heat shock protein beta-1 (also known as heat shock protein 27 [*Hsp27*]). Regulation of *Hspb1*/*Hsp27* transcription is known to be controlled by *Atf5* (activating transcription factor 5).[122] In our study *Atf5* was transcriptionally increased at day 1 postdetachment, and a subsequent rise in *Hspb1*/*Hsp27* transcript levels was seen by day 7 postdetachment.

Perhaps the most striking example of a temporal correlation between an increased transcription factor level followed by target gene increases is with the STAT1 gene. Our microarray data show that *Stat1* shows increased transcription as early as day 1 postdetachment, a finding that has been independently observed in other studies. The family of STAT transcription factors is pivotal in the regulation of multiple cytokine pathways, including that of interleukin-6 and ciliary neurotrophic factor in the retina.[123,124] At day 7 postdetachment, our microarray data show a marked increase in transcript levels for interferon-inducible genes. In fact, 9 interferon-inducible genes were observed to have increased transcript levels at this time point (*Ifi27l*, *Ifi30*, *Ifitm1_predicted*, *Ifitm2*, *Ifitm3*, *Ifngr1*, *Ifngr2_predicted*, *Irf1*, *Irf7*). STAT1 is a major regulator of interferon signaling and the transcriptional control of interferon-inducible genes.[125] Our data suggest that STAT1 regulates the downstream transcription of these interferon-pathway genes after retinal detachment. The interferon-mediated pathway has been implicated as having a possible anti-apoptotic role in other models of retinal disease, and assessing its role in the physiology of the detached retina provides an intriguing area for further research.

In more chronic detachments such as studied in our 28-day postdetachment samples, the gene transcription profile of the retina shows differential expression of a much smaller number of genes than in the 7-day postdetachment samples. As expected, there were markedly fewer transcription factors being differentially expressed at this later time point. Instead, there was higher differential expression of genes that fall into diverse categories such as immune system genes (complement components, Fc receptors), lysosomal proteins (cathepsin C, S, and Z), protease inhibitors (*A2m*, *Serpina3n*, *Serpin1*), and cytoskeleton/cellular-remodeling proteins (*Gfap*, *Timp1*), to name a few. As mentioned previously, we detected increased *Gfap* transcript levels at all 3 time points tested. This finding is consistent with the previously demonstrated protein data[32-34] and serves as an independent internal validation of the microarray results.

An unexpected finding in our microarray data was the large number of genes differentially expressed in detached retinas that can be categorized as immune-response genes. Retinal detachment does not typically trigger an inflammatory reaction, in the sense that there is not a large influx of white cells into the retina. Macrophages have been shown to infiltrate into the retina after retinal detachment, but this appears to be more of a response to the immune-response genes activated from within the retina rather than the source of the immune signals.[126] Genes coding for immune-response proteins, particularly complement factors, have recently been implicated in modulating the response of the retina in other diseases, such as age-related macular degeneration.[127-129] Immune response genes have also been demonstrated to play a large role in response to oxidative stress in a number of systems.[130,131] Müller and other microglial cells are known to undergo multiple morphologic and functional transformations after retinal detachment and would seem to be likely modulators or sources of many of these transcriptionally up-regulated genes. More work is required to define the role these various genes play in the response of the retina to detachment and whether modulation of these responses would improve retinal function after repair of the detachment. Also, the role these genes play in controlling some of the secondary consequences of retinal detachment, such as proliferative vitreoretinopathy, needs to be elucidated.

Metabolism genes undergo large changes in transcription after retinal detachment. Retinal detachment, by definition, involves separation of the retina from a major source of its metabolic support (ie, the RPE). As such, the changes in metabolism gene transcription represent an expected response to the altered homeostasis of the retina. In addition to directly altering metabolism, cells can respond to nutritional deprivation by activating autophagy pathways.[132,133] Autophagy (literally "eating of oneself") is a process by which cells induce the endosomal or lysosomal recycling of unwanted, damaged, or redundant components. This may occur as a part of a cell's normal damage repair system, but can also occur as a response to starvation or stress. Under these latter conditions, autophagy recycles scarce resources for more vital functions related to cell survival. Thus, activation of autophagy often represents a "cell survival" mechanism. In our microarray analysis, there were significant increases in the transcription of lysosome-related genes. In other systems, activation of these genes represents indirect evidence of autophagy activation. The study of autophagy in retinal disease has been very limited, and more work needs to be done to define the role autophagy plays in the survival of retinal cells during periods of stress or injury (as represented by retinal detachment in this study).

The 3×2 ANOVA analysis looking at the effect of time of detachment (1 day, 7 days, 28 days) vs detachment state (attached vs detached) reveals 100 genes showing differential expression. These genes fall into similar categories as the genes found on the individual day analyses. Fewer genes show significance in their transcription level when analyzed across time owing to the large variations that were seen for some genes at an individual time point, or if they were highly differentially expressed at all 3 time points (ie, they didn't "vary" across time). Reducing the analysis to a 2×2 ANOVA, with only the days 1 and 7 postdetachment time points, increases the number of genes with significant differential expression to 144. This is because the day 28 microarray analysis shows higher variability than the earlier time points. This higher variability is not necessarily unexpected, owing to the intrinsic variability of such a complex biological system and with analysis of gene transcription levels coming from multiple cell lines in various states of postinjury degeneration. As such, the ANOVA analyses are highlighting the genes with the most significant changes in transcription levels and do not negate the validity of the individual day results.

The validation of transcript changes with qRT-PCR showed that the gene with the highest increase in transcription was that for lipocalin 2 (*Lcn2*). Lipocalins are proteins that bind low-molecular-weight ligands.[134] Their functions are varied, depending on the ligand they bind. Lipocalin 2 is also known as neutrophil gelatinase–associated lipocalin and is thought to be an iron-binding protein. Lipocalin 2 has been shown to be an acute phase reactant, and urinary levels of this protein can be measured using a commercially available diagnostic marker for acute renal disease. In kidney epithelium, lipocalin 2 mediates iron trafficking. Lipocalin 2 does not bind iron directly, but rather binds the siderophore enterochelin, which has bound the iron. Iron is an important cofactor for numerous enzymes, and lipocalin 2 can serve as a modulator of these enzymatic reactions through the regulation of iron transport. Increased lipocalin 2 expression has been observed in Müller cells of rats with streptozotocin-induced diabetes.[135] Lipocalin 2 transcript levels were previously found to be increased in mouse retinas transiently detached by subretinal injection of saline.[136] Iron-mediated toxicity has recently been implicated as a contributor to retinal damage in age-related macular degeneration and hereditary retinal degenerations, presumably through oxidative stress.[137-139] Our data also show increased transcript levels for ceruloplasmin, ferritin light chain 1 and metallothionein 1A and 2A (Table 2). These genes are involved in divalent metal ion regulation, particularly iron and zinc.[140] Cumulatively, these data could represent an intrinsic response to iron-mediated (and possibly zinc-mediated) toxicity in the oxidative stress that occurs during retinal detachment.

A novel gene whose markedly increased transcript level was confirmed with qRT-PCR was that encoding for galanin (*Gal*). Galanin is a 29–amino acid peptide that is found in many tissues. Galanin acts predominantly as a neurotransmitter and exerts its actions by binding to one of three G protein–coupled receptor subtypes.[141] Its function depends on the specific tissue within which it is expressed and receptor to which it binds. In experimental models of nerve injury, however, there are significant increases of both galanin gene transcription and levels of secreted peptide. In these models, galanin is thought to play a neuroprotective role and may serve to enhance nerve cell survival and potentially even regeneration. Within the retina, galanin has been found to play a role in retinal development,[142] but little is known about its role in response to injury in the fully developed eye and this requires further study.

The initiation of transcription in response to retinal detachment requires detection of the altered homeostasis by the retina. The signal(s) that initiate these events remain unclear as does the type of retinal cell(s) that transduce these signals. Oxygen tension has been shown to be severely reduced in the photoreceptor layer of the detached retina,[143,144] and oxygen supplementation has been shown to limit some of the morphologic changes that occur in the detached retina.[37-40] There is an increase in cytotoxic amino acids recovered from the subretinal space of detached retinas,[80,145] suggesting that perhaps they contribute to the initiation of altered transcription. Another possible signaling molecule is the chromophore of the visual pigment found in the photoreceptor cells themselves (ie, retina). After absorption of light, the retinal chromophore is released from the opsin molecule. The retina normally undergoes reprocessing through a complex series of enzymatic reactions in the retinal and underlying RPE, a process known as the visual cycle or vitamin A cycle. This normal process is clearly disrupted during retinal detachment, and the outer retina and subretinal space become bathed in an excess of released chromophore. Our microarray data show increased transcription within the retina of several genes that control vitamin A processing (retinol binding protein 1/*Rbp1*, retinol dehydrogenase 10/*Rdh10*, retinol dehydrogenase 11/*Rdh11*, and retinal pigment epithelium 65/*RPE65*). The clearance of such a highly reactive oxidative molecule (retinal) after injury is another area that requires further study.

Transduction of stress stimuli often occurs through the MAP kinase pathway.[118-120] Our results show early activation of the p42/p44 subgroup of MAP kinases. Activation of this subgroup, also known as the ERK family of MAP kinases, is often associated with cellular response to stress.[118] As shown in our data, the activation of this molecule occurs by phosphorylation of a preexisting pool of these proteins, allowing the cells to respond very quickly to the altered homeostasis. In our model, we detected phosphorylated p42/p44 kinase as early as 2 hours after retinal-RPE separation, suggesting that activation of these molecules can act as an early trigger for the altered transcription that is detected at later time points. Other signaling pathways may also be responding to the altered homeostasis, and these need to be defined. Furthermore, the actual trigger(s) to which these pathways are reacting need to be more clearly elucidated, as well as the specific role these pathways play in effecting the gene transcription changes described earlier. As these are very early molecular responses to the separation of the retina from the RPE, preventing MAP kinase activation can serve as a potential point of intervention for modulating downstream cellular response and reducing unwanted consequences that occur after retinal detachment.

In summary, complex genetic and biochemical changes occur within the cells of the retina in response to separation from the RPE. This work helps define some of the transcriptional changes and early stress-response pathways that become activated in response to the altered retinal homeostasis. Areas that require particular emphasis in future studies are defining the specific signals that initiate activation of these pathways; ascertaining the specific retinal cell types within which these different transcriptional changes are occurring; and further characterizing the role the differentially expressed genes play in the morphologic and functional changes that

occur after retinal detachment. The results described in this thesis lay the groundwork for these future studies, the results of which will allow for a better understanding of how to intervene at the molecular level to improve visual outcomes for patients with retinal disease.

## ACKNOWLEDGMENTS

Funding/Support: This work was supported by grant K08-EY-14705 from the National Eye Institute and a Career Development Award from Research to Prevent Blindness, Inc.

Financial Disclosures: None.

Conformity With Author Information: All animal experiments were performed in accordance with the ARVO Statement for the Use of Animals in Ophthalmic and Vision Research and the guidelines established by the University Committee on Use and Care of Animals of the University of Michigan.

Other Acknowledgments: The author wishes to acknowledge the work of David Reed, PhD, for help with the statistical analysis; Ying Han, MD, and P. William Conrad, MD, PhD, for technical help with the experiments; and Richard Hackel for his help in preparing the figures. All these persons are from the Department of Ophthalmology and Visual Sciences, University of Michigan.

## REFERENCES

1. Miller RF. The physiology and morphology of the vertebrate retina. In: Ogden TE, Hinton DR, eds. *Retina*. 3rd ed. St Louis: CV Mosby; 2001:138-170.
2. Pournaras CJ, Rungger-Brandle E, Riva CE, Hardarson SH, Stefannson E. Regulation of retinal blood flow in health and disease. *Prog Retin Eye Res* 2008;27:284-330.
3. Wangs-Wirawan ND, Linsenmeier RA. Retinal oxygen: fundamental and clinical aspects. *Arch Ophthalmol* 2003;121:547-557.
4. Gonin J. La pathogénie du décollement spontané del at rétine. *Ann d'Oculist (Paris)* 1904;132:30.
5. Young LHY, D'Amico DJ. Retinal detachment. In: Albert DM, Jakobiec FA, Azar DT, Gragoudas ES, eds. *Principles and Practice of Ophthalmology*. 2nd ed. Philadelphia: WB Saunders; 2000:2352-2358.
6. Fisher SK, Anderson DH. Cellular effects of detachment on the neural retina and the retinal pigment epithelium. In: Ogden TE, Hinton DR, eds. *Retina*. 3rd ed. St Louis: Mosby; 2001:1961-1986.
7. Kenneth NS, Rocha S. Regulation of gene expression by hypoxia. *Biochem J* 2008;414:19-29.
8. Van Elzen R, Moens L, Dewilde S. Expression profiling of the cerebral ischemic and hypoxic response. *Expert Rev Proteiomics* 2008;5:263-282.
9. Mathers J, Fraser JA, McMahon M, Saunders RD, Hayes JD, McLellan LI. Antioxidant and cytoprotective responses to redox stress. *Biochem Soc Symp* 2004;71:157-176.
10. Sen B, Mahadevan B, DeMarini DM. Transcriptional responses to complex mixtures: a review. *Mutat Res* 2007;636:144-177.
11. Machemer R, Norton EW. Experimental retinal detachment in the owl monkey. I. Methods of production and clinical picture. *Am J Ophthalmol* 1968;66:388-395.
12. Machemer R. Experimental retinal detachment in the owl monkey. II. Histology of the retina and pigment epithelium. *Am J Ophthalmol* 1968;66:396-410.
13. Kroll AJ, Machemer R. Experimental retinal detachment in the owl monkey. III. Electron microscopy of retina and pigment epithelium. *Am J Ophthalmol* 1968;66:410-427.
14. Kroll AJ, Machemer R. Experimental retinal detachment in the owl monkey. V. Electron microscopy of the reattached retina. *Am J Ophthalmol* 1969;67:117-130.
15. Kroll AJ, Machemer R. Experimental retinal detachment and reattachment in the rhesus monkey. Electron microscopic comparison of rods and cones. *Am J Ophthalmol* 1969;68:58-77.
16. Kroll AJ. Secondary retinal detachment. Electron microscopy of retina and pigment epithelium. *Am J Ophthalmol* 1969;68:223-237.
17. Machemer R, Kroll AJ. Experimental retinal detachment in the owl monkey. VII. Photoreceptor protein renewal in normal and detached retina. *Am J Ophthalmol* 1971;71:690-695.
18. Kroll AJ, Machemer R. Experimental retinal detachment in the owl monkey. VIII. Photoreceptor protein renewal in early retinal reattachment. *Am J Ophthalmol* 1971;72:356-366.
19. Anderson DH, Stern WH, Fisher SK, Erickson PA, Borgula GA. The onset of pigment epithelial proliferation after retinal detachment. *Invest Ophthalmol Vis Sci* 1981;21:10-16.
20. Lewis GP, Sethi CS, Linberg KA, Charteris DG, Fisher SK. Experimental retinal detachment. A new perspective. *Mol Neurobiol* 2003;28:159-175.
21. Fisher SK, Lewis GP, Linberg KA, Verardo MR. Cellular remodeling in mammalian retina: results from studies of experimental retinal detachment. *Prog Retin Eye Res* 2005;24:395-431.
22. Williams DS, Fisher SK. Prevention of rod disk shedding by detachment from the retinal pigment epithelium. *Invest Ophthalmol Vis Sci* 1987;28:184-187.
23. Guerin CJ, Anderson DH, Fariss RN, Fisher SK. Retinal reattachment of the primate macula. Photoreceptor recovery after short-term detachment. *Invest Ophthalmol Vis Sci* 1989;30:1708-1725.

24. Guerin CJ, Lewis GP, Fisher SK, Anderson DH. Recovery of photoreceptor outer segment length and analysis of membrane assembly rates in regenerating primate photoreceptor outer segments. *Invest Ophthalmol Vis Sci* 1993;34:175-183.
25. Cook B, Lewis GP, Fisher SK, Adler R. Apoptotic photoreceptor degeneration in experimental retinal detachment. *Invest Ophthalmol Vis Sci* 1995;36:990-996.
26. Lewis GP, Linberg KA, Fisher SK. Neurite outgrowth from bipolar and horizontal cells after experimental retinal detachment. *Invest Ophthalmol Vis Sci* 1998;39:424-434.
27. Fisher SK, Lewis GP. Muller cell and neuronal remodeling in retinal detachment and reattachment and their potential consequences for visual recovery: a review and reconsideration of recent data. *Vision Res* 2003;43:887-898.
28. Fisher SK, Erickson PA, Lewis GP, Anderson DH. Intraretinal proliferation induced by retinal detachment. *Invest Ophthalmol Vis Sci* 1991;32:1739-1748.
29. Guerin CJ, Anderson DH, Fisher SK. Changes in intermediate filament immunolabeling occur in response to retinal detachment and reattachment in primates. *Invest Ophthalmol Vis Sci* 1990;31:1474-1482.
30. Lewis GP, Matsumoto B, Fisher SK. Changes in the organization and expression of cytoskeletal proteins during retinal degeneration induced by retinal detachment. *Invest Ophthalmol Vis Sci* 1995;36:2404-2416.
31. Lewis GP, Fisher SK. Muller cell outgrowth after retinal detachment: association with cone photoreceptors. *Invest Ophthalmol Vis Sci* 2000;41:1542-1545.
32. Lewis GP, Erickson PA, Guerin CJ, Anderson DH, Fisher SK. Changes in the expression of specific Muller cell proteins during long-term retinal detachment. *Exp Eye Res* 1989;49:93-111.
33. Erickson PA, Feinstein SC, Lewis GP, Fisher SK. Glial fibrillary acidic protein and its mRNA: ultrastructural detection and determination of changes after CNS injury. *J Struct Biol* 1992;108:148-161.
34. Lewis GP, Guerin CJ, Anderson DH, Matsumoto B, Fisher SK. Rapid changes in the expression of glial cell proteins caused by experimental retinal detachment. *Am J Ophthalmol* 1994;118:368-376.
35. Lewis GP, Erickson PA, Guerin CJ, Anderson DH, Fisher SK. Basic fibroblast growth factor: a potential regulator of proliferation and intermediate filament expression in the retina. *J Neurosci* 1992;12:3968-3978.
36. Lewis GP, Linberg KA, Geller SF, Guerin CJ, Fisher SK. Effects of the neurotrophin brain-derived neurotrophic factor in an experimental model of retinal detachment. *Invest Ophthalmol Vis Sci* 1999;40:1530-1544.
37. Lewis G, Mervin K, Valter K, et al. Limiting the proliferation and reactivity of retinal Müller cells during experimental retinal detachment: the value of oxygen supplementation. *Am J Ophthalmol* 1999;128:165-172.
38. Mervin K, Valter K, Maslim J, Lewis G, Fisher S, Stone J. Limiting photoreceptor death and deconstruction during experimental retinal detachment: the value of oxygen supplementation. *Am J Ophthalmol* 1999;128:155-164.
39. Lewis GP, Talaga KC, Linberg KA, Avery RL, Fisher SK. The efficacy of delayed oxygen therapy in the treatment of experimental retinal detachment. *Am J Ophthalmol* 2004;137:1085-1095.
40. Sakai T, Lewis GP, Linberg KA, Fisher SK. The ability of hyperoxia to limit the effects of experimental retinal detachment in cone dominated retina. *Invest Ophthalmol Vis Sci* 2001;42:3264-3273.
41. Geller SF, Lewis GP, Fisher SK. FGFR1, signaling, and AP-1 expression after retinal detachment: reactive Müller and RPE cells. *Invest Ophthalmol Vis Sci* 2001;42:1363-1369.
42. Kroemer G, Petit P, Zamzami N, Vayssiere JL, Mignotte B. The biochemistry of programmed cell death. *FASEB J* 1995;9:1277-1287.
43. Oppenheim RW. Cell death during development of the nervous system. *Ann Rev Neurosci* 1991;14:453-501.
44. Nickells RW, Zack DJ. Apoptosis in ocular disease: a molecular overview. *Ophthalmic Gen* 1996;17:145-165.
45. Lipton SA, Rosenberg PA. Excitatory amino acids as a final common pathway for neurologic disorders. *N Engl J Med* 1994;330:613-622.
46. Kerr JFR, Wyllie AH, Currie AR. Apoptosis: a basic biological phenomenon with wide-ranging implications in tissue kinetics. *Br J Cancer* 1972;26:239-257.
47. Kroemer G, Zamzami N, Susin SA. Mitochondrial control of apoptosis. *Immunol Today* 1997;18:44-51.
48. Nickells RW. Apoptosis of retinal ganglion cells in glaucoma: an update of the molecular pathways involved in cell death. *Surv Ophthalmol* 1999;43(Supp1):S151-161.
49. Osborne NN, Ugarte M, Chao M, et al. Neuroprotection in relation to retinal ischemia and relevance to glaucoma. *Surv Ophthalmol* 1999;43(Supp1):S102-128.
50. Schwartz M, Belkin M, Yoles E, Solomon A. Potential treatment modalities for glaucomatous neuropathy: neuroprotection and neuroregeneration. *J Glaucoma* 1996;5:427-432.
51. Dreyer EB, Pan ZH, Storm S. Greater sensitivity of larger retinal ganglion cells to NMDA-mediated cell death. *Neuroreport* 1994;5:629-631.
52. Brooks DE, Garcia GA, Dreyer EB, Zurakowski D, Franco-Bourland RE. Vitreous body glutamate concentration in dogs with glaucoma. *Am J Vet Res* 1997;58:864-867.
53. Vorwerk CK, Gorla MSR, Dreyer EB. An experimental basis for implicating excitotoxicity in glaucomatous optic neuropathy. *Surv Ophthalmol* 1999;43(Supp1):S142-150.
54. Vorwerk CK, Lipton SA, Zurakowski D, Hyman BT, Sabel BA, Dreyer EB. Chronic low dose glutamate is toxic to retinal ganglion cells: toxicity blocked by memantine. *Invest Ophthalmol Vis Sci* 1996;37:1618-1624.

55. Sucher NJ, Lipton SA, Dreyer EB. Molecular basis of glutamate toxicity in retinal ganglion cells. *Vision Res* 1997;37:3483-3493.
56. Pease ME, McKinnon SJ, Quigley HA, Kerrigan-Baumrind LA, Zack DJ. Obstructed axonal transport of BDNF and its receptor TrkB in experimental glaucoma. *Invest Ophthalmol Vis Sci* 2000;41:764-774.
57. Farkas RH, Grosskreutz CL. Apoptosis, neuroprotection and retinal ganglion cell death: an overview. *Int Ophthalmol Clin* 2001;41:111-130.
58. Xu GZ, Li WWY, Tso MOM. Apoptosis in human retinal degenerations. *Trans Am Ophthalmol Soc* 1996;94:411-430.
59. Reme CE, Grimm C, Hafezi F, Marti A, Wenzel A. Apoptotic cell death in retinal degenerations. *Prog Retin Eye Res* 1998;17:443-464.
60. Travis GH. Mechanisms of cell death in the inherited retinal degenerations. *Am J Hum Genet* 1998;62:503-508.
61. Wen R, Song Y, Cheng T, et al. Injury-induced upregulation of bFGF and CNTF mRNAs in the rat retina. *J Neurosci* 1995;15:7377-7385.
62. Wen R, Cheng T, Li Y, Cao W, Steinberg RH. Alpha 2-adrenergic agonists induce basic fibroblast growth factor expression in photoreceptors in vivo and ameliorate light damage. *J Neurosci* 1996;16:5986-5992.
63. LaVail MM, Yasumura D, Matthes ME, Lau-Villacorta C, Sung CH, Steinberg RH. CNTF delays photoreceptor degeneration in rd and Q344ter mutant rhodopsin transgenic mice. *Invest Ophthalmol Vis Sci* 1996;37:2007.
64. LaVail MM, Yasumura D, Matthes MT, et al. Protection of mouse photoreceptors by survival factors in retinal degenerations. *Invest Ophthalmol Vis Sci* 1998;39:592-602.
65. LaVail MM. Legacy of the RCS rat: impact of a seminal study on retinal cell biology and retinal degenerative disease. *Prog Brain Res* 2001;131:617-627.
66. Bush RA, Lei B, Tao W, et al. Encapsulated cell-based intraocular delivery of ciliary neurotrophic factor in normal rabbit: dose-dependent effects on ERG and retinal histology. *Invest Ophthalmol Vis Sci* 2004;45:2420-2430.
67. Sieving PA, Caruso RC, Tao W, et al. Ciliary neurotrophic factor (CNTF) for human retinal degeneration: phase I trial of CNTF delivered by encapsulated cell intraocular implants. *Proc Natl Acad Sci U S A* 2006;103:3896-3901.
68. Chen J, Flannery JG, LaVail MM, Steinberg RH, Xu J, Simon MI. bcl-2 Overexpression reduces apoptotic photoreceptor cell death in three different retinal degenerations. *Proc Natl Acad Sci U S A* 1996;93:7042-7047.
69. Hafezi F, Steinbach JP, Marti A, et al. The absence of c-fos prevents light-induced apoptotic cell death of photoreceptors in retinal degeneration in vivo. *Nat Med* 1997;3:346-349.
70. Nir I, Kedzierski W, Chen J, Travis GH. Expression of Bcl-2 protects against photoreceptor degeneration in retinal degeneration slow (rds) mice. *J Neurosci* 2000;20:2150-2154.
71. Hobson AH, Donovan M, Humphries MM, et al. Apoptotic photoreceptor death in the rhodopsin knockout mouse in the presence and absence of c-fos. *Exp Eye Res* 2000;71:247-254.
72. Wenzel A, Grimm C, Seelinger MW, et al. Prevention of photoreceptor apoptosis by activation of the glucocorticoid receptor. *Invest Ophthalmol Vis Sci* 2001;42:1653-1659.
73. Donovan M, Carmody RJ, Cotter TG. Light-induced photoreceptor apoptosis in vivo requires nNOS and guanylate cyclase activity and is caspase-3 independent. *J Biol Chem* 2001;276:23000-23008.
74. Nakajima M, Yuge K, Senzaki H, et al. Photoreceptor apoptosis induced by a single systemic administration of N-methyl-N-nitrosourea in the rat retina. *Am J Pathol* 1996;148:631-641.
75. Yoshizawa K, Yang J, Senzaki H, et al. Caspase-3 inhibitor rescues N-methyl-N-nitrosourea–induced retinal degeneration in Sprague-Dawley rats. *Exp Eye Res* 2000;71:629-635.
76. Stone J, Maslim J, Valter-Kocsi K, et al. Mechanisms of photoreceptor death and survival in mammalian retina. *Prog Retin Eye Res* 1999;18:689-735.
77. Hisatomi T, Sakamoto T, Murata T, et al. Relocalization of apoptosis inducing factor in photoreceptor apoptosis induced by retinal detachment in vivo. *Am J Pathol* 2001;158:1271-1278.
78. Zacks DN, Hanninen V, Pantcheva M, Ezra E, Grosskreutz C, Miller JW. Caspase activation in an experimental model of retinal detachment. *Invest Ophthalmol Vis Sci* 2003;44:1262-1267.
79. Chang CJ, Lai WW, Edward DP, Tso MO. Apoptotic photoreceptor cell death after traumatic retinal detachment in humans. *Arch Ophthalmol* 1995;113:880-886.
80. Marc RE, Murry RF, Fisher SK, Linberg KA, Lewis GP. Amino acid signatures in the detached cat retina. *Invest Ophthalmol Vis Sci* 1998;39:1694-1702.
81. Walczak H, Krammer PH. The CD95 (APO-1/Fas) and the TRAIL (APO-2L) apoptosis systems. *Exp Cell Res* 2000;256:58-66.
82. Barnhart BC, Alappat EC, Peter ME. The CD95 type I/type II model. *Semin Immunol* 2003;15:185-193.
83. Loeffler M, Kroemer G. The mitochondrion in cell death control: certainties and incognita. *Exp Cell Res* 2000;256:19-26.
84. Zacks DN, Zheng QD, Han Y, Bakhru R, Miller JW. FAS-mediated apoptosis and its relation to intrinsic pathway activation in an experimental model of retinal detachment. *Invest Ophthalmol Vis Sci* 2004;45:4563-4569.
85. Yang L, Bula D, Arroyo JG, Chen DF. Preventing retinal detachment-associated photoreceptor cell loss in bax-deficient mice. *Invest Ophthalmol Vis Sci* 2004;45:648-654.
86. Harrison DC, Davis RP, Bond BC, et al. Caspase mRNA expression in a rat model of focal cerebral ischemia. *Mol Brain Res* 2001;89:133-146.

87. Krupinski J, Lopez E, Marti E, Ferrer I. Expression of caspases and their substrates in the rat model of focal cerebral ischemia. *Neurobiol Dis* 2000;7:332-342.
88. Rosenbaum DM, Gupta G, D'Amore J, et al. Fas (CD95/APO-1) plays a role in the pathophysiology of focal cerebral ischemia. *J Neurosci Res* 2000;61:686-692.
89. Zacks DN, Boehlke C, Richards AL, Zheng QD. Role of the Fas-signaling pathway in photoreceptor neuroprotection. *Arch Ophthalmol* 2007;125:1389-1395.
90. Erickson PA, Fisher SK, Anderson DH, Stern WH, Borgula GA. Retinal detachment in the cat: the outer nuclear and outer plexiform layers. *Invest Ophthalmol Vis Sci* 1983;24:927-942.
91. Cobb JP, O'Keefe GE. Injury research in the genomic era. *Lancet* 2004;363:2076-2083.
92. Zhang KH, Xiao HS, Lu PH, et al. Differential gene expression after complete spinal cord transaction in adult rats: an analysis focused on a subchronic post-injury stage. *Neuroscience* 2004;128:375-388.
93. Abankwa D, Kury P. Traumatic injury to CNS fiber tracts–what are the genes telling us? *Curr Drug Targets* 2004;5:647-654.
94. Price RM, Tulsyan N, Dermody JJ, Schwalb M, Soteropoulos P, Castronuovo JJ Jr. Gene expression after crush injury of human saphenous vein: using microarrays to define the transcriptional profile. *J Am Coll Surg* 2004;199:411-418.
95. Vazueez-Chona F, Song BK, Geisert EE Jr. Temporal changes in gene expression after injury in the rat retina. *Invest Ophthalmol Vis Sci* 2004;45:2737-2746.
96. Chen L, Wu W, Dentchev T, et al. Light damage induced changes in mouse retinal gene expression. *Exp Eye Res* 2004;79:239-247.
97. Lo WR, Rowlette LL, Caballero M, Yang P, Hernandez MR, Borras T. Tissue differential microarray analysis of dexamethasone induction reveals potential mechanisms of steroid glaucoma. *Invest Ophthalmol Vis Sci* 2003;44:473-485.
98. Zacks DN, Han Y, Zeng Y, Swaroop A. Activation of signaling pathways and stress-response genes in an experimental model of retinal detachment. *Invest Ophthalmol Vis Sci* 2006;25:205-208.
99. Xu FH, Sharma S, Gardner A, et al. Interleukin-6-induced inhibition of multiple myeloma cell apoptosis: support for the hypothesis that protection is mediated via inhibition of the JNK/SAPK pathway. *Blood* 1998;92:241-251.
100. Chauhan D, Kharbanda S, Ogata A, et al. Interleukin-6 inhibits FAS-induced apoptosis and stress-activated protein kinase activation in multiple myeloma cells. *Blood* 1997;89:227-234.
101. Bansal MB, Kovalovich K, Gupta R, et al. Interleukin-6 protects hepatocytes from CCl(4)-mediated necrosis and apoptosis in mice by reducing MMP-2 expression. *J Hepatol* 2005;42:548-556.
102. Taub R. Hepatoprotection via the IL-6/Stat3 pathway. *J Clin Invest* 2003;112:978-980.
103. Kovalovich K, Li W, DeAngelis R, Greenbaum LE, Ciliberto G, Taub R. Interleukin-6 protects against FAS-mediated death by establishing a critical level of anti-apoptotic hepatic proteins FLIP, Bcl-2, and Bcl-xL. *J Biol Chem* 2001;276:26605-26613.
104. Heinrich PC, Behremann I, Haan S, Hermanns HM, Muller-Newen G, Schaper F. Principles of interleukin (IL)-6-type cytokine signaling and its regulation. *Biochem J* 2003;374:1-20.
105. Yamashita T, Sawamoto K, Suzuki S, et al. Blockade of interleukin-6 signaling aggravates ischemic cerebral damage in mice: possible involvement of Stat3 activation in the protection of neurons. *J Neurochem* 2005;94:459-468.
106. Sanchez RN, Chan CK, Kwong GS, Wong MJ, Sadun AA, Lam TT. Interleukin-6 in retinal ischemia reperfusion injury in rats. *Invest Ophthalmol Vis Sci* 2003;44:4006-4011.
107. Inomata Y, Hirata A, Yonemura N, Koga T, Kido N, Tanihara H. Neuroprotective effects of interleukin-6 on NMDA-induced rat retinal damage. *Biochem Biophys Res Commun* 2003;302:226-232.
108. Maier K, Rau CR, Storch MK, et al. Ciliary neurotrophic factor protects retinal ganglion cells from secondary cell death during acute autoimmune optic neuritis in rats. *Brain Pathol* 2004;14:378-387.
109. van Adel BA, Arnold JM, Phipps J, Doering LC, Ball AK. Ciliary neurotrophic factor protects retinal ganglion cells from axotomy-induced apoptosis via modulation of retinal glia in vivo. *J Neurobiol* 2005;63:215-234.
110. Chong DY, Boehlke CS, Zheng QD, Zhang L, Han Y, Zacks DN. Interleukin-6 as a photoreceptor neuroprotectant in an experimental model of retinal detachment. *Invest Ophthalmol Vis Sci* 2008;49:3193-3200.
111. Wilson CL, Miller CJ. Simpleaffy: BioConductor package for Affymetrix quality control and data analysis. *Bioinformatics* 2005;21:3683-3685.
112. Simon R, Lam A, Li M-C, Ngan M, Menenzes S, Zhao Y. Analysis of gene expression data using BRB-Array tools. *Cancer Inform* 2007;2:11-17.
113. Wright G, Simon R. A random variance model for detection of differential gene expression in small micro-array experiments. *Bioinformatics* 2003;19:2448-2455.
114. Saldanha AJ. Treeview-extensible visualization of micro-array data. *Bioinformatics* 2004;20:3246-3248.
115. Draghici S, Khatri P, Tarca AL, et al. A systems biology approach for pathway level analysis. *Genome Res* 2007;17:1537-1545.
116. Pawitan Y, Michiels S, Koscielny S, Gusnanto A, Ploner A. False discovery rate, sensitivity and sample size for microarray studies. *Bioinformatics* 2005;21:3017-3024.
117. Hayes MJ, Moss SE. Annexins and disease. *Biochem Biophys Res Commun* 2004;322:1166-1170.
118. Rubinfeld H, Seger R. The ERK cascade: a prototype of MAPK signaling. *Mol Biotechnol* 2005;31:151-174.
119. Roux PP, Blenis J. ERK and p38 MAPK-activated protein kinases: a family of protein kinases with diverse biological functions. *Microbiol Mol Biol Rev* 2004;68:320-344.
120. Turjanski AG, Vaque JP, Gutkind JS. MAP kinases and the control of nuclear events. *Oncogene* 2007;26:3240-3253.

121. Allan AL, Albanes C, Pestell RG, LaMarre J. Activating transcription factor 3 induces DNA synthesis and expression of Cyclin D1 in hepatocytes. *J Biol Chem* 2001;276:27272-27280.
122. Wang H, Lin G, Zhang Z. ATF5 promotes cell survival through transcriptional actvation of Hsp27 in H9c2 cells. *Cell Biol Int* 2007;31:1309-1315.
123. Rhee KD, Goureau O, Chen S, Yang XJ. Cytokine-induced activation of signal transducer and activator of transcription in photoreceptor precursors regulates rod differentiation in the developing mouse retina. *J Neurosci* 2004;24:4081-4090.
124. Peterson WM, Wang Q, Txekova R, Wiegand SJ. Ciliary neurotrophic factor and stress simuli activate the Jak-STAT pathway in retinal neurons and glia. *J Neurosci* 2000;20:4081-4090.
125. Brierley MM, Fish EN. Stats: multifaceted regulators of transcription. *J Interferon Cytokine Res* 2005;25:733-744.
126. Nakazawa T, Hisatomi T, Nakazawa C, et al. Monocyte chemoattractant protein 1 mediates retinal detachment-induced photoreceptor apoptosis. *Proc Natl Acad Sci U S A* 2007;104:2425-2430.
127. Nussenblatt RB, Ferris F 3rd. Age-related macular degeneration and the immune response: implications for therapy. *Am J Ophthalmol* 2007;144:618-626.
128. Coffey PJ, Gias C, McDermott CJ, et al. Complement factor H deficiency in aged mice causes retinal abnormalities and visual dysfunction. *Proc Natl Acad Sci U S A* 2007;104:16651-16656.
129. Hollyfield JG, Bonilha VL, Rayborn ME, et al. Oxidative damage-induced inflammation initiates age-related macular degeneration. *Nat Med* 2008;14:194-198.
130. Pockley AG, Muthana M, Calderwood SK. The dual immunoregulatory roles of stress proteins. *Trends Biochem Sci* 2008;33:71-79.
131. Skaper SD. The brain as a target for inflammatory processes and neuroprotective strategies. *Ann N Y Acad Sci* 2007;1122:23-34.
132. Galluzzi L, Vicencio JM, Kepp O, Tasdemir E, Maiuri MC, Kroemer G. To die or not to die: that is the autophagic question. *Curr Mol Med* 2008;8:78-91.
133. Vicencio JM, Galluzzi L, Tajeddine N, et al. Senescence, apoptosis or autophagy? When a damaged cell must decide its path. *Gerontology* 2008;54:92-99.
134. Schmidt-Ott KM, Mori K, Kalandadze A, et al. Neutrophil gelatinase-associated lipocalin-mediated iron traffic in kidney epithelia. *Curr Opin Nephrol Hypertens* 2006;15:442-449.
135. Gerhardinger C, Costa MB, Coulombe MC, Toth I, Hoehn T, Grosu P. Expression of acute-phase response proteins in retinal Muller cells in diabetes. *Invest Ophthalmol Vis Sci* 2005;46:349-357.
136. Farjo R, Peterson WM, Naash MI. Expression profiling after retinal detachment and reattachment: a possible role for aquaporin-0. *Invest Ophthalmol Vis Sci* 2008;49:511-521.
137. Loh A, Hadziahmetovic M, Dunaief JL. Iron homeostasis and eye disease. *Biochim Biophys Acta* 2009;1790:637-649.
138. Wong RW, Richa C, Hahn P, Green WR, Dunaief JL. Iron toxicity as a potential factor in AMD. *Retina* 2007;27:997-1003.
139. Deleon E, Lederman M, Berenstein E, Meir T, Chevion M, Chowers I. Alteration in iron metabolism during retinal degeneration in rd10 mouse. *Invest Ophthalmol Vis Sci* 2009;50:1360-1365.
140. Dutsch-Wicherek M, Sikora J, Tomaszewska R. The possible biological role of metallothionein in apoptosis. *Front Biosci* 2008;13:4029-4038.
141. Lang R, Gundlach AL, Kofler B. The galanin peptide family: receptor pharmacology, pleitropic biological actions, and implications in health and disease. *Pharmacol Ther* 2007;115:177-207.
142. Xu ZQ, Shi TJ, Hokfelt T. Expression of galanin and a galanin receptor in several sensory systems and bone anlage of rat embryos. *Proc Natl Acad Sci U S A* 1996;93:14901-14905.
143. Linsenmeier RA, Padnick-Silver L. Metabolic dependence of photoreceptors on the choroid in the normal and detached retina. *Invest Ophthalmol Vis Sci* 2000;41:3117-3123.
144. Wang S, Linsenmeier RA. Hyperoxia improves oxygen consumption in the detached feline retina. *Invest Ophthalmol Vis Sci* 2007;48:1335-1341.
145. Bertram KM, Bula DV, Pulido JS, et al. Amino-acid levels in subretinal and vitreous fluid of patients with retinal detachment. *Eye* 2008;22:582-589.